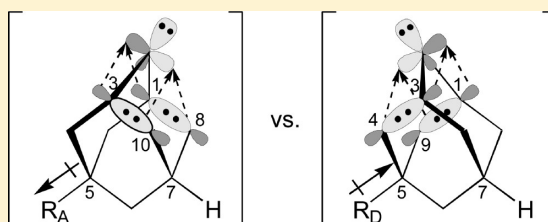


Intra- and Intermolecular Reaction Selectivities of γ -Substituted AdamantanylidenesWolfgang Knoll,[‡] Daisuke Kaneno,[§] Michael M. Bobek,[‡] Lothar Brecker,[‡] Murray G. Rosenberg,[‡] Shuji Tomoda,[§] and Udo H. Brinker^{*‡}[‡]Chair of Physical Organic and Structural Chemistry, Institute of Organic Chemistry, University of Vienna, Währinger Strasse 38, A-1090 Vienna, Austria[§]Department of Life Sciences, Graduate School of Arts and Sciences, The University of Tokyo, 3-8-1 Komaba, Meguro-Ku, Tokyo 153-8902, Japan

S Supporting Information

ABSTRACT: A study of adamantanylidenes having a γ -substituent (R) was undertaken to gauge how inductive and steric effects of remotely positioned functional groups influence intra- and intermolecular product selectivity. 3H-Diazirines were thermolyzed or photolyzed to generate the corresponding carbenes. On rapid heating, the resulting carbenes isomerized to 2,4-didehydroadamantanes by intramolecular 1,3-CH insertions. When R was an electron donor (R_D) mostly asymmetric 1-substituted derivatives were produced but when it was an electron acceptor (R_A) the symmetric 7-substituted ones were formed.

When solutions were exposed to UV-A light, intermolecular adducts from the carbenes and solvent predominated with lesser amounts of intramolecular product being formed. Valence isomerization of 3H-diazirines also afforded diazo compounds. In methanol, protonation of diazo compounds to give the corresponding 2-adamantyl cations exceeds their coupling. This diversion was controlled with fumaronitrile by trapping the diazo compounds. The adducts possessed mostly *anti* configurations with $R = R_D$ and *syn* arrangements with $R = R_A$. The connection between *as*- and *anti*-product formation and that of *s*- and *syn*-products was deemed to be the consequence of a rapid equilibrium between two distinct carbene conformations. This was qualified and quantified using ab initio calculations and NBO analyses.



INTRODUCTION

X-Functionalized adamantanylidenes¹ bearing a remotely positioned γ -substituent (R; cf. Figure 1) have long intrigued

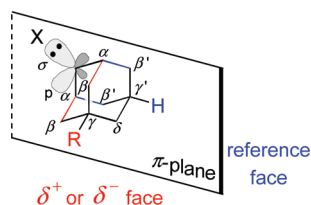


Figure 1. X-functionalized adamantanylidenes.

physical organic chemists because an unexpected and unexplained bias toward one of two possible isomeric addition products is observed.² π -Facial selectivities of γ -substituted methylenadamantanes ($X = CH_2$),³ adamantanones (4, $X = O$),² and 2-adamantyl cations (6, $X = H^+$)⁴ are well documented. It has been suggested that partially charged (δ^\pm) R groups guide the approaching reagent, e.g., a nucleophile (Nu), by external electrostatic interaction, but the considerable distance between R and C–X putatively excludes Coulombic effects and steric hindrance as factors.⁵ Instead, the pendant group is widely believed to govern reactivity through internal

stereoelectronic effects.⁶ The Cieplak and Felkin–Anh models are two competing proposals that predict *opposite* selectivities based on the inductive (I) nature of R,⁷ which can be either an electron donor (R_D) or acceptor (R_A). They claim that stereoselection is due to σ -bond I effects and antiperiplanar MO hyperconjugation during the bond-forming transition state (TS; cf. Figure 2).⁸ Indeed, the latter effect is quite pronounced

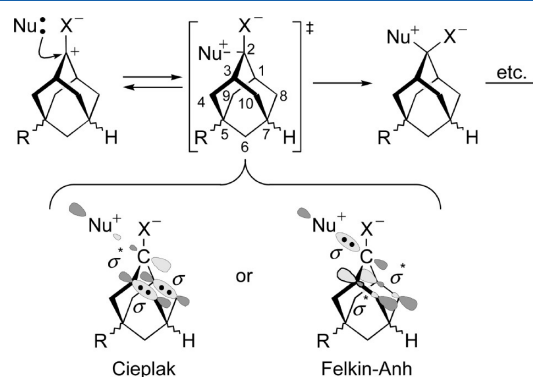


Figure 2. Representation of the Felkin–Anh and the Cieplak model.

Received: October 17, 2011

Published: December 14, 2011

with **4** despite the Felkin–Anh model being deemed inappropriate for the adamantanyl system by its founder.⁹ However, strong arguments assert that both models demonstrate which π -face deters Nu–C formation rather than which one promotes it.

In any case, theoretical chemistry was used to discredit the TS models in Figure 2,¹⁰ which were also found to be inadequate for reactive intermediates.^{11–13} Given this conundrum, dismissing the outer effects of R in the ground state (GS) may have been premature.

X-functionalized adamantanylidene with a γ -substituent (R; X = O, CH₂, H⁺, etc.) undergo nucleophilic addition reactions that exhibit π -facial diastereoselectivity depending on the inductive effect of R, cf. R_D and R_A. However, this bias has not been properly explained by MO theory. So, despite being far from the CX bond, Coulombic interaction and steric hindrance by R have been reconsidered. Note that the CX bond orbital in the general molecule is drawn to highlight the underlying carbene (cf. Figure 1).

As a nucleophile (Nu = O, CBr₂, H⁺, etc.) approaches the electrophilic sp²-hybridized C-2 atom of an X-functionalized γ -substituted adamantanylidene (X = O, CH₂, H⁺, etc.), the incipient Nu···C-2 MO of the reactant-like activated complex is thought to hyperconjugate with those of the antiperiplanar C- α –C- β bonds on the opposite face of the molecule. The linearly combined MO interaction presumably lowers the energy of the participating electron-pair through delocalization, so the early TS is stabilized and the rate of isomer formation increases. Two opposing hypotheses of the TS have been proposed to explain stereoselective bond formation. In the Cieplak model, the σ^* -ABMO of Nu···C-2 interacts with the better donating C- α –C- β σ -BMO on the substituted face when R = R_D. Thus, the addition product in which R and Nu are anti is favored. When R = R_A, interaction of the Nu···C-2 σ^* -ABMO is greater with the higher-energy C- α –C- β' σ -BMO on the reference face. So, a preference for the product wherein R and Nu are syn is expected. In the Felkin–Anh model, the σ -BMO of Nu···C-2 interacts with the better accepting C- α –C- β' σ^* -ABMO on the reference face if R = R_D. So, the adduct having R and Nu configured syn predominates. When R = R_A, better hyperconjugation of the Nu···C-2 σ -BMO with the lower energy C- α –C- β σ^* -ABMO on the substituted face leads mostly to the product with R and Nu situated anti to one another. Thus, these two models make opposite predictions.

The exterior frontier orbital extension (EFOE) model can be used to evaluate how much R affects an incoming reagent.¹³ It is based on the first and last terms of the Salem–Klopman equation,¹⁴ which divides the net reaction energy (ΔE) into three parts: (1) the exchange repulsion (steric) term, (2) the electrostatic interaction (Coulombic) term, and (3) the donor–acceptor MO interaction term. The π -plane divided accessible space (PDAS; cf. Figure 1) within 2.65 Å of each molecular face is calculated to quantify the steric effect of R on the CX-bond. Then the EFOE electron density of each PDAS around the C–X FMO is calculated to determine the orbital's distortion index (δ), which is related to the activation enthalpy (ΔH^\ddagger). The difference in ΔH^\ddagger for each TS ($\Delta\Delta H^\ddagger \neq 0$) usually accounts for product selectivity, which may be plotted as ln(isomer ratio).

For example, the PDAS (cf. Figure 1) of ketone **4** is rendered unequal when R \neq H and the course of reaction is thereby influenced.¹³ Hydride reduction of ketone **4h** with NaBH₄ yields a modest ratio (ca. 1.5:1) of the corresponding alcohols.¹⁵ However, ratios approach 9:1 for cation **6h** (Figure 3).⁴ The marked

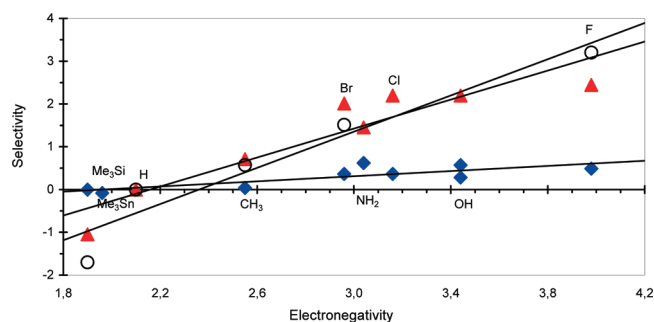


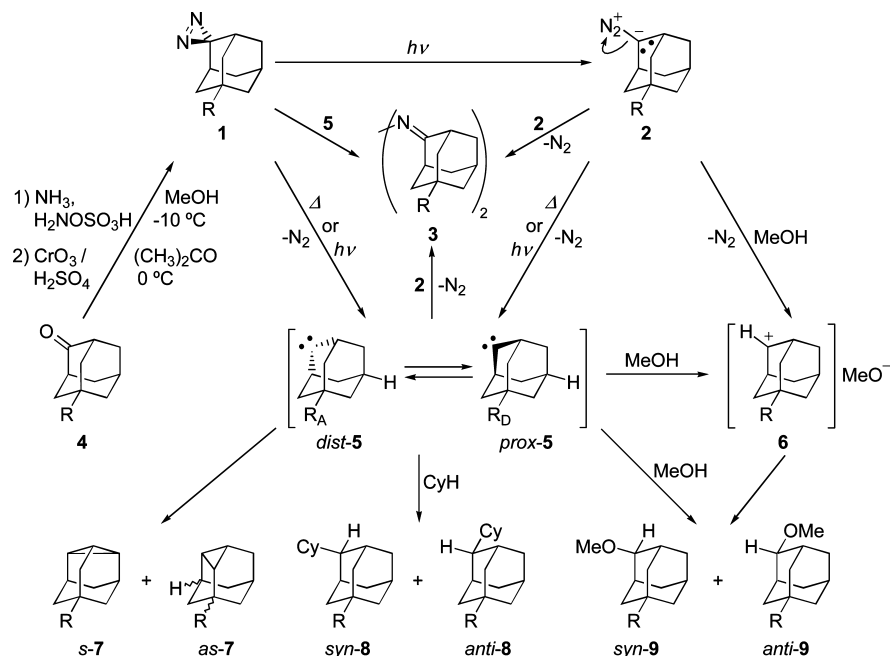
Figure 3. There is a linear relationship between product selectivity, expressed as ln(isomer ratio), and the *I* effect of R (◆: hydride reduction of γ -substituted adamantanones; ▲: intramolecular 1,3-CH insertion reaction of γ -substituted adamantanylidene; ○: reaction of γ -substituted 2-adamantyl cations).

selectivity of **6** has been attributed to hyperconjugation,^{16,17} which is maximized when σ -bond *I* effects stemming from R cause the α -bridge to bend toward (*proximal*) or away from (*distal*) the γ -substituent. Thus, access to one face of the CX-bond is physically restricted and product ratios are concomitantly altered. If the difference in ΔH^\ddagger for each TS is negligible, i.e., $\Delta\Delta H^\ddagger \approx 0$, then product distribution must be dictated by an energy difference between two separate minima inhabited by distinct conformers,^{15b,16} i.e., *prox-6* and *dist-6*.

A similar situation might exist with the isoelectronic carbene **5**, which is different from carbenium ion **6** in two key ways. First, the influence of Coulombic charge is absent with neutral carbene **5**. Second, adamantanylidene reacts intramolecularly by 1,3-CH insertion. Thus, both intra- and intermolecular selectivities may be studied. And, even though the selectivities of reactions with different molecularities cannot be easily compared, certain conclusions may be drawn by simply comparing the TSs and their energies in relation to the energies of the corresponding carbene conformers. Therefore, advanced computational methods, like density functional theory (DFT) ab initio MO calculations, that properly reflect experimental results should help to pinpoint the source of reaction selectivity. Indeed, the analysis of adamantane-related intermediates should be possible using natural bond orbital (NBO) theory,¹⁸ because it has already been used to investigate the effect of double-hyperconjugation on 4-substituted cyclohexyl cations.¹⁹ The following is a report on the experimental intramolecular regioselectivities and intermolecular stereoselectivities of the bare γ -substituted adamantanylidene **5**,^{20–22} i.e., the ephemeral carbenes *without* X. The dynamic origins of these reciprocal selectivities are examined using computational methods.

RESULTS AND DISCUSSION

The intramolecular regioselectivity of α -substituted adamantanylidene giving 1- and 3-substituted 2,4-didehydroadamantanes has been studied.²⁰ In that case, the proximity of R to the divalent C atom likely obfuscates *I* effects with steric ones. With γ -substituted adamantanylidene,²³ that should not be the case. So, this report focuses only on such adamantanylidene, building upon earlier work.^{12,21,24} During hydride reduction of ketones **4**,^{2,5a} the γ -substituents exert different σ -bond inductive effects.²⁵ Therefore, various functional groups covering a wide range of electronegativity values were sought. The Me₃Si group served as an undisputed R_D when compared with H,²⁶ i.e., the reference “group.” And F was used for its pronounced effects as an R_A. The Me group was also chosen, because its behavior as

Scheme 1. Generation of Conformationally Equilibrated γ -Substituted Adamantanylidenes and Their Subsequent Reactions^a

^aR = SiMe₃ (a), H (b), Me (c), NH₂ (d), OH (e), Br (f), Cl (g), F (h).

an R_D or R_A has been in dispute for a long time.²⁷ This ancillary issue was investigated through experimental product ratios and NBO analysis as well.

There is a broad variety of carbene precursors available,²⁸ but 3H-diazirines **1** were chosen as the most appropriate ones for carbenes **5**.^{23a,29,30} Scheme 1 outlines the preparation of 3H-diazirine **1**, from the corresponding ketone **4**, and its response to heat (Δ) and light ($h\nu$). Labile **1** either expels N₂ to directly generate short-lived carbene **5** or it isomerizes to diazo compound **2**, which can be a problematic diversion. During photolysis,³¹ 3H-diazirine **1b** forms an unstable mixture of carbene **5b** (40%) and diazo compound **2b** (60%). Continued photolysis of **2b** does generate **5b**. Depending on solution concentration and acidity, however, dipolar **2** can couple with itself to form inert azines **3**.³² This lowers the overall yield of carbene **5**, which is shown rapidly equilibrating between distal (*dist-5*) and proximal (*prox-5*) conformations. These two distinct conformational isomers undergo either intramolecular isomerization to 2,4-didehydroadamantanes **7** or intermolecular addition with solvent. In aprotic cyclohexane (CyH), insertion into a C–H bond leads to **8**. In protic methanol (MeOH), however, OH-insertion predominates and **9** is formed.

Under thermal conditions,^{22,33} aziadamantane (**1b**) almost exclusively generates the corresponding carbene **5b**, which isomerizes to 2,4-didehydroadamantane (**7b**). Cyclopropane formation from 1,3-CH insertion is a signature reaction of carbenes. Here, it is the only intramolecular transformation possible^{22b} because the vicinal migrating hydride orbitals are orthogonal to the p-LUMO centered on the electrophilic divalent carbon (cf. Figure 4a). Moreover, a 1,2-H shift would produce adamantene, which is an anti-Bredt alkene destabilized by a twisted double-bond ($E_{\text{strain}} = 39$ kcal/mol).³⁴

Adamantanone tosylhydrazone salts form carbenes under thermal conditions ($T = 130$ – 140 °C).²⁰ Indeed, they were used to first generate adamantanylidene (**5b**).^{22a} The intramolecular 1,3-CH insertion reaction of carbene **5b** is both experimentally and

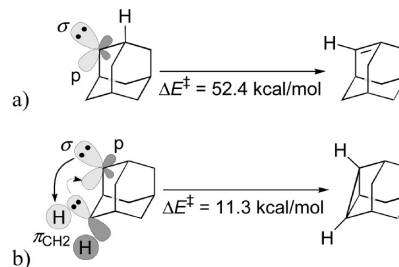


Figure 4. Relative energies for (a) 1,2-H shift and (b) 1,3-CH insertion calculated at the B3LYP/6-311++G(3df,2pd)//B3LYP/6-31+G(d) level of theory.^{22b}

theoretically well investigated. In fact, the selectivity of substituted derivatives has been used to support Cieplak's TS model.^{5a} Gas-phase pyrolysis of γ -substituted aziadamantanes **1** were conducted in this account to generate didehydroadamantanes **7**. Regioisomer ratios (except **7c**, see Experimental Section) were determined from integrated analytical GC signals (cf. Table 1).

Table 1. Ratios of Intramolecular 1,3-CH Insertion Products Obtained by the Gas-Phase Pyrolysis of Aziadamantanes **1**

reactant	R	<i>s-7</i>	<i>as-7</i>	ratio
1a	Me ₃ Si	27	73	1:2.7
1c	Me	66	34	1.9:1
1d	NH ₂	81	19	4.3:1
1e	OH	89	11	8.1:1
1f	Br	89	11	8.1:1
1g	Cl	90	10	9.0:1
1h	F	92	8	11.5:1

They show that the formation of 7-substituted 2,4-didehydroadamantanes (*s-7*), i.e., carbene insertion into a reference-face C–H bond, is strongly preferred for compounds bearing an R_A. The most pronounced effect was observed with F-substituted

Table 2. Energy of Carbene 5 Conformers and Their Intermediary TS

carbene	bridge tilt ^a (deg)	GS E (hartree)	$\Delta E_{dist-5 \rightarrow prox-5}$ (kcal/mol)	TS E (hartree)	$\Delta E^{\ddagger b}$ (kcal/mol)
<i>prox-5a</i>	−15.21	−798.0950	−0.44	−798.0940	0.59
<i>dist-5a</i>	+13.34	−798.0943			0.19
5b	±15.07	−389.4101		−389.4093	0.52
<i>prox-5c</i>	−14.0	−428.7294	0.63	−428.7291	0.18
<i>dist-5c</i>	+15.70	−428.7304			0.81
<i>prox-5d</i> (C _s)	−11.86	−444.7659	1.00	−444.7658	0.08
<i>dist-5d</i> (C _s)	+16.69	−444.7675			1.14
<i>prox-5d</i> (C ₁)	−13.6	−444.7656	1.26	−444.7656	0.00
<i>dist-5d</i> (C ₁)	+16.51	−444.7676			1.24
<i>prox-5e</i> (C _s)	−13.38	−464.6336	1.44	−464.6336	0.00
<i>dist-5e</i> (C _s)	+17.06	−464.6359			1.44
<i>prox-5h</i>	−12.97	−488.6565	1.88	−488.6566	0.00
<i>dist-5h</i>	+17.35	−488.6595			1.85

^aThe dihedral angle is measured from the C-1–C-6–C-3 plane; (+) denotes distal from R and (−) signifies proximal to R. ^bActivation energy for conformer interconversion: $\Delta E^{\ddagger} = E_{TS} - E_{GS}$. Calculated at the B3LYP/6-31+G(d,p) level of theory.

carbenes *dist*- and *prox-5h*, which form *s*- and *as-7h* in a ratio of 92:8. Formation of 1-substituted 2,4-didehydroadamantanes (*as-7*), i.e., insertion into a C–H bond on the substituted face, was favored only with the R_D Me₃Si (*s-7a/as-7a* = 27:73). The inverted isomeric product ratio appears to indicate a reversal in the lower energy conformation of carbene **5**, which was investigated using computational methods.

Accurate structures of carbenes **5** were attained by geometry optimization using high-level ab initio calculations. Carbenes **5** were found to be more stable when their C-1–C-2–C-3 α -bridges were bent toward the C- α –C- β bonds (cf. Figure 5).

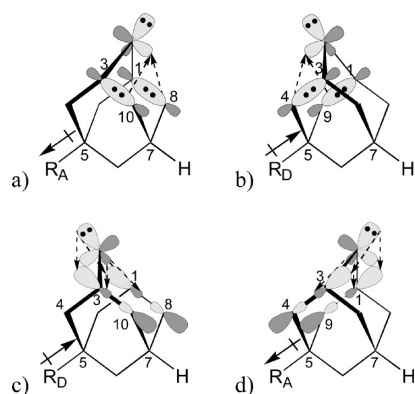


Figure 5. Stabilization of bent γ -substituted adamantanylenes **5**. Cieplak-type (a and b) and Felkin–Anh-type (c and d) orbital interactions reinforce one another in the GS and determine the major carbene conformer. (Note: For the less stable minor conformers, swap the R_D and R_A labels in a–d, because the donor face acts as acceptor and the acceptor face as donor.)

This is true even for unsubstituted **5b**,^{22b} which is most stable when its divalent-carbon bridge is bent $\pm 15.07^\circ$ from center (cf. Table 2). Thus, the C_{2v}-symmetric TS(**5b** \rightleftharpoons **5b**) (cf. Scheme 1) represents the unperturbed carbene bridge, which swings between two turning points. This rapid dynamic entails two equivalent GS minima separated by a TS that is 0.50 kcal/mol higher in energy. For γ -substituted adamantanylenes, both minima are not isoenergetic and the difference reveals the influence of R. There is some concern about how this thermodynamic interchange might affect the multiplicity of carbene **5**. The parent **5b** was assumed to have a triplet ground state (T₀), like other dialkylcarbenes, until it was found to have

a singlet ground state (S₀).³⁵ But the calculated S₀–T₀ energy gap is relatively small (ca. 2.8 kcal/mol).^{22b,36} Those for **5a** (2.8 kcal/mol) and **5h** (2.3 kcal/mol) are comparable to this.

NBO analysis of the carbene **5** conformer pairs and their intervening TS suggests that tilting of the α -bridge has two principal causes (cf. Figure 5). One is a ground-state Cieplak-type interaction involving electron-donation from a collinear C- α –C- β σ -BMO to the nominally empty p-LUMO (lp*) of the divalent C atom.^{37,38} Indeed, NBO analyses of lp* show that it is partially occupied (cf. Table 3). This is due to electron-donation from a C- α –C- β σ -BMO, i.e., Cieplak-type interaction. The other cause is a ground-state Felkin–Anh-type interaction, which involves electron-donation by the filled σ -HOMO (lp) of the divalent C atom to a synperiplanar C- α –C- β σ^* -ABMO. This contribution is somewhat less pronounced, presumably because the Cieplak-type interaction involves electron-donation from two filled orbitals to one empty one whereas Felkin–Anh-type stabilization entails hyperconjugation from one filled orbital to two empty ones (cf. Figure 5). Nevertheless, both MO interactions are greater than those in the TS (**5** \rightleftharpoons **5**) (cf. Scheme 1). By bending, carbene **5** better aligns its orthogonal σ - and p-FMO with the C- α –C- β (anti)bonds thereby maximizing hyperconjugation on both faces. Not only can these donor–acceptor MO interactions be visualized (cf. Figure 6)—they can be quantified as well (cf. Table 3). When R \neq H, there is a preferred bending direction that depends on the I effect of R. This leads to two distinct conformers with regard to R, i.e., *dist*- and *prox-5*. The structures of parent **5b**, TMS-substituted *dist*- and *prox-5a*, and F-substituted *dist*- and *prox-5h* were theoretically determined and used as prime examples. Figure 7 shows the structures of *dist*- and *prox-5a*, **5b**, *dist*- and *prox-5c*, and *dist*- and *prox-5h*. It includes diagnostic parameters: E, ZPVE, and bending angle. Table 2 lists ground state (GS) and TS energies as well as the kinetic barriers of interconversion between *dist-5* and *prox-5*.

There are two conformers of carbene **5**, i.e., proximal and distal with regard to R, because α -bridge bending can occur in either direction. The major conformation is lower in energy than the minor one; the amount of interaction between the p- and σ -FMOs centered on C-2 and the C- α –C- β BMO and ABMO, respectively, determines which is which. With an R_D, such as Me₃Si, *prox-5* is more stable than *dist-5*. There are two reasons. First, the lp* achieves better overlap with the better donating C- α –C- β σ -BMO on the substituted face

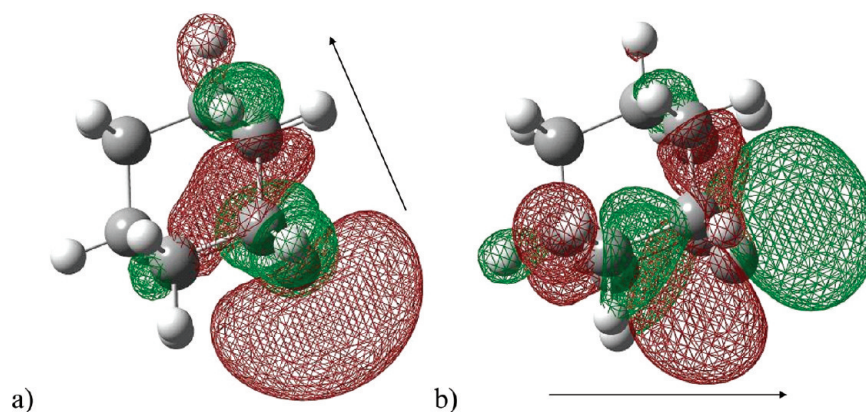


Figure 6. Contour plots of the (a) HOMO and (b) LUMO of carbene **5b**. The arrows indicate donor–acceptor electron-delocalization. FMO energies of carbenes **5** are listed in Table 4.

Table 3. NBO Stabilization Energies for Carbenes **5**

structure	$\Delta E_{dist-5 \rightarrow s}$ (kcal/mol)	lp (e^-) ^a	lp* (e^-) ^b	Cieplak-type ΔE^c (kcal/mol)	Felkin–Anh-type ΔE^d (kcal/mol)	total ΔE^e (kcal/mol)
<i>prox-5a</i>	−0.44	1.9099	0.20	12.3	6.6	37.8
<i>dist-5a</i>		1.9108	0.19	11.0	6.3	34.6
5b		1.91	0.186	11.9	6.5	36.9
TS(5b → 5b)		1.92	0.16	5.1	2.9	31.8
<i>prox-5h</i>	1.88	1.917	0.159	10.2	5.7	31.8
<i>dist-5h</i>		1.911	0.187	13.1	7.1	40.4

^aElectron occupancy of carbene **5** HOMO or corresponding C atom in the TS. ^bElectron occupancy of carbene **5** LUMO or corresponding C atom in the TS. ^cInteraction energies between lp* and one of two C- α –C- β σ -BMO donors. These are C- α –C- β (C-1–C-9 and C-3–C-4) for *prox-5* and C- α –C- β' (C-1–C-8 and C-3–C-10) for *dist-5*. ^dInteraction energies between lp and one of two C- α –C- β σ^* -ABMO acceptors. These are C- α –C- β' (C-1–C-8 and C-3–C-10) for *prox-5* and C- α –C- β (C-1–C-9 and C-3–C-4) for *dist-5*. ^eThe sum of all relevant ΔE s.

(cf. Cieplak-type interaction; Figure 5a). Second, the lp overlaps better with the better accepting C- α –C- β' σ^* -ABMO on the reference face (cf. Felkin–Anh-type interaction; Figure 5c). With an R_A, like F, *dist-5* is lower in energy than *prox-5*. In this case, stabilization is better achieved when the lp* overlaps with the higher-energy C- α –C- β' σ -BMO on the reference face (cf. Cieplak-type interaction; Figure 5b) and the lp overlaps with the lower energy C- α –C- β σ^* -ABMO on the substituted face (cf. Felkin–Anh-type interaction; Figure 5d). Thus, in contrast to nucleophilic addition of X-functionalized γ -substituted adamantanylenes (cf. Figure 2), the *ground-state* Cieplak- and Felkin–Anh-type interactions are collaborative. The dependence on R is revealed in Figure 8 and Figure 9.

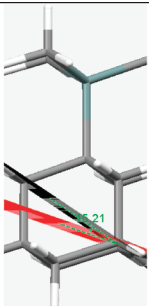
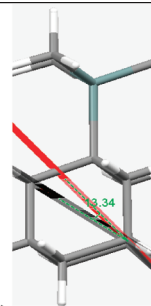
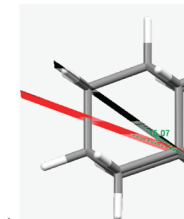
The carbene **5** conformational energy difference ($\Delta E_{dist-5 \rightarrow prox-5}$) depends on the *I* effect of R. When R = R_D, *prox-5* is the major conformer. When R = R_A, *dist-5* predominates. Note that there is a reversal in the preferred conformation when R is an R_D versus when it is an R_A. Carbenes **5d** and **5e** can exist as different rotational isomers. The C₁- and C_s-symmetric rotamers lead to two data sets (cf. Table 2 and Table 3). Carbenes **5f** and **5g** exhibit deviations, because their halogen substituents have similar *I* effects but different valence shells.

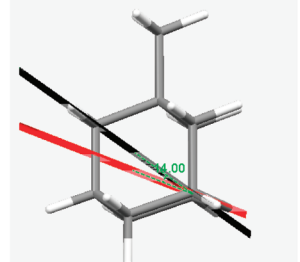
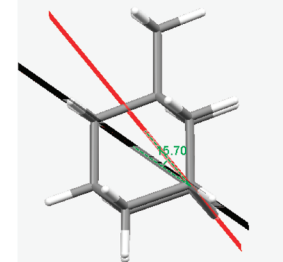
The γ -substituent of carbene **5** affects its FMO energies (cf. Figure 9 and Table 4). The general appearance and shape of the HOMO and LUMO are shown in Figure 6. An R_A group withdraws electron density from the remote divalent C atom thereby enhancing its electrophilicity. The HOMO and LUMO energy levels are lowered, i.e., become more negative (cf. Figure 9). The opposite may be said for R_D groups. Although the HOMO levels of **5** are affected by the *I* effect of R, they are barely influenced by which direction the α -bridge is bending;

the energy values for *prox-* and *dist-5* are approximately the same. On the other hand, the LUMO levels are influenced by R and the conformation. Indeed, the proximal carbenes are affected more than the distal ones. These findings are in accordance with the effects of hyperconjugation, which affect the p-LUMO, cf. Cieplak-type interaction, more than the σ -HOMO, cf. Felkin–Anh-type. Thus, the major carbene **5** conformer is mainly determined by the amount of electron-donation to its LUMO.

Thus far, all of the results indicate that the Me group is an R_A when compared with the H atom reference group. Moreover, NBO analyses of 5-methyladamantan-2-ylidenes *dist-5c* and *prox-5c* agree with the findings. They were used to estimate interaction energies between C- γ –CH₃ and the relevant C- α –C- β bond. The interaction energy with C- γ –CH₃ as acceptor and one of the C- α –C- β bonds on the substituted face (2.37 kcal/mol for *dist-5c* and 2.31 kcal/mol for *prox-5c*) was greater than that with C- γ –CH₃ as donor (1.79 kcal/mol for the major conformer *dist-5c* and 1.93 kcal/mol for the minor conformer *prox-5c*). The C- γ' –H bond on the reference face behaves contrarily. As an acceptor, the interaction energies are 1.92 kcal/mol for *dist-5c* and 1.97 kcal/mol for *prox-5c*. But they are greater as a donor: 2.92 kcal/mol for *dist-5c* and 2.73 kcal/mol for *prox-5c*.

When compared with that for typical alkanylenes, the ΔE^\ddagger for intramolecular 1,3-CH insertion of carbene **5** to didehydroadamantane **7** is higher (13 kcal/mol; cf. Figure 4). This considerable TS barrier confers two experimental advantages: (1) compounds *s-7* and *as-7* are conveniently obtained as the main products of thermal gas-phase reactions, and (2) they are formed only as minor byproducts during liquid-phase solution photolyses. The calculated activation entropy (ΔS^\ddagger) for

 <p>a)</p>	 <p>b)</p>	 <p>c)</p>
<i>prox-5a</i> -798.095 15.21° 199.261 -0.40	<i>dist-5a</i> -798.094 13.34° 198.647 —	5b -389.410 15.07° 135.99 —

 <p>d)</p>	 <p>e)</p>
<i>prox-5c</i> -428.729 14.00° 153.248 0.630	<i>dist-5c</i> -428.730 15.70° 153.260 —

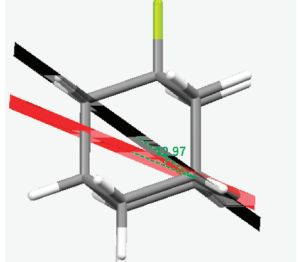
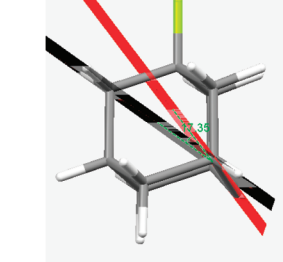
 <p>f)</p>	 <p>g)</p>
<i>prox-5h</i> -488.657 12.97° 130.726 1.915	<i>dist-5h</i> -488.659 17.35° 130.942 —

Figure 7. Structures of carbenes *dist-5a*, *prox-5a*, **5b**, *dist-5c*, *prox-5c*, *dist-5h*, and *prox-5h* with selected parameters: *E* (hartree), bending angle (deg), ZPVE (kcal/mol), $\Delta E_{dist-5 \rightarrow prox-5}$ (kcal/mol; (–) exothermic vs (+) endothermic.

TS(*S* → *7*) is negative (from –2 to –3 cal/(mol·K)), which indicates a particularly ordered unimolecular TS. The energy differences between TS(*prox-5* → *as-7*) and TS(*dist-5* → *s-7*) were calculated and found to roughly parallel $\Delta E_{dist-5 \rightarrow prox-5}$ (cf. Table 2 and Table 5), although slightly increasing with increasing substituent electronegativity. This implies that the ΔE^\ddagger for the 1,3-CH insertion in carbene **5** depends somewhat on its conformation.

The ratio of intramolecular products **7** from carbenes **5** depends on the activation free energy (ΔG^\ddagger) values qualitatively depicted in Figure 10. For a rapid equilibrium, $\Delta G^\ddagger(b)$ and $\Delta G^\ddagger(c)$ are small. Therefore, their difference is small and usually ignored. Indeed, the Curtin–Hammett principle³⁹ states that the product ratio depends only on $\Delta G^\ddagger(d) - \Delta G^\ddagger(a)$, i.e., k_d/k_a . However, the solution to the rate equations reveals greater flexibility. Here, the position of the carbene **5** conformational

equilibrium, which is reflected by the sign and magnitude of $\Delta G^\circ(f)$, would be the main source of 1,3-CH insertion regioselectivity.

As noted, Figure 10 illustrates transient carbene **5** in rapid conformational equilibrium between distal and proximal forms that interconvert through a TS that is *C*_{2v}-symmetric in **5b**, i.e., R = H. The lower energy conformer depends on the direction of inductive effects of γ -substituent R. Each conformer isomerizes to a preferred intramolecular regioisomer **7** and the product ratio mostly reflects the relative populations of the carbene conformers *prox-5* and *dist-5*. In solution, intermolecular reaction (not shown) predominates exhibiting stereoselectivity that is also R-dependent. The energies of the lowest vibrational energy levels within each minimum were determined in order to make zero-point vibrational energy (ZPVE) corrections to ΔE values.

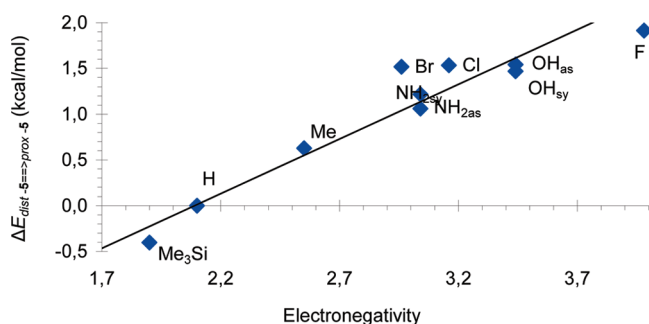


Figure 8. Conformational energy difference of substituted adamantanylenes **5** vs the electronegativity of the substituent.

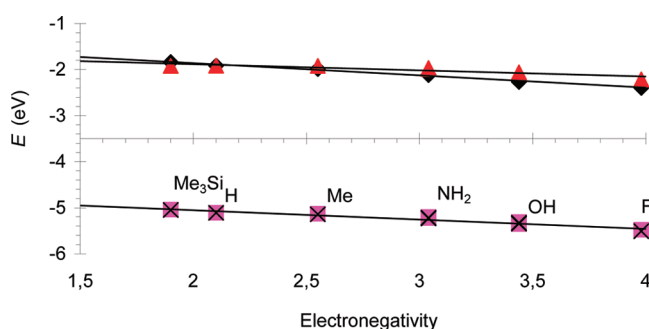


Figure 9. Energy of the frontier orbitals of substituted adamantanylenes **5** vs the electronegativity of the substituent. The *I* effect of R within carbene **5** affects the energy of frontier molecular orbitals (■: *prox-5* HOMO; ◆: *prox-5* LUMO; ×: *dist-5* HOMO; ▲: *dist-5* LUMO).

Table 4. Frontier Molecular Orbital Energies

carbene	E_{HOMO} (eV)	E_{LUMO} (eV)
<i>prox-5a</i>	−5.0407	−1.8406
<i>dist-5a</i>	−5.0485	−1.9229
5b	−5.1098	−1.9199
<i>prox-5c</i>	−5.1321	−1.9882
<i>dist-5c</i>	−5.1419	−1.9243
<i>prox-5d</i> (C_1)	−5.2243	−2.1087
<i>dist-5d</i> (C_1)	−5.2324	−1.9863
<i>prox-5d</i> (C_s)	−5.1998	−2.1179
<i>dist-5d</i> (C_s)	−5.2189	−1.9672
<i>prox-5e</i> (C_1)	−5.3114	−2.2680
<i>dist-5e</i> (C_1)	−5.3277	−2.0608
<i>prox-5e</i> (C_s)	−5.3525	−2.2550
<i>dist-5e</i> (C_s)	−5.3468	−2.0821
<i>prox-5h</i>	−5.4794	−2.3973
<i>dist-5h</i>	−5.5087	−2.2171

Ab initio computations do confirm that the insertion $\Delta\Delta E^\ddagger$ for *prox-* and *dist-5* is not zero. So, although facial selectivity is mainly determined by the relative populations of the carbene conformers *prox-5* and *dist-5*, it is partially influenced by each conformer's intrinsic ability to react. The magnitude of α -bridge-bending and resulting stabilization for the major carbene **5** conformer is always marginally greater than that for the minor one (cf. Figure 11). And as the *I* effect of R strengthens with respect to the H atom reference, there is a slight increase in energy difference between the carbene **5** conformers

Table 5. Effect of the γ -Substituent on the Energy of TS (**5** \rightarrow **7**)

TS	ZPVE (kcal/mol)	E (hartree)	ΔE^a (kcal/mol)
<i>prox-5a</i> \rightarrow <i>as-7a</i>	197.9771	−798.0752	−1.08
<i>dist-5a</i> \rightarrow <i>s-7a</i>	198.0467	−798.0736	
5b \rightarrow 7b	134.8502	−389.3896	
<i>prox-5c</i> \rightarrow <i>as-7c</i>	152.0577	−428.7092	0.51
<i>dist-5c</i> \rightarrow <i>s-7c</i>	152.0114	−428.7099	
<i>prox-5g</i> \rightarrow <i>as-7g</i>	128.8329	−848.9880	1.97
<i>dist-5g</i> \rightarrow <i>s-7g</i>	128.8852	−848.9912	
<i>prox-5h</i> \rightarrow <i>as-7h</i>	129.5381	−488.6356	2.14
<i>dist-5h</i> \rightarrow <i>s-7h</i>	129.6684	−488.6392	

$$^a \Delta E = E_{\text{TS}(\text{prox-5} \rightarrow \text{as-7})} - E_{\text{TS}(\text{dist-5} \rightarrow \text{s-7})}$$

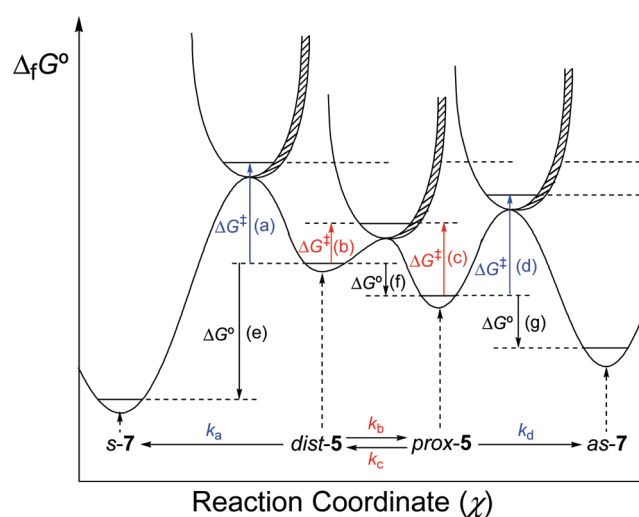


Figure 10. Curtin–Hammett-type energy profile (not to scale) showing saddle points where the GS surface meets orthogonal TS surfaces.

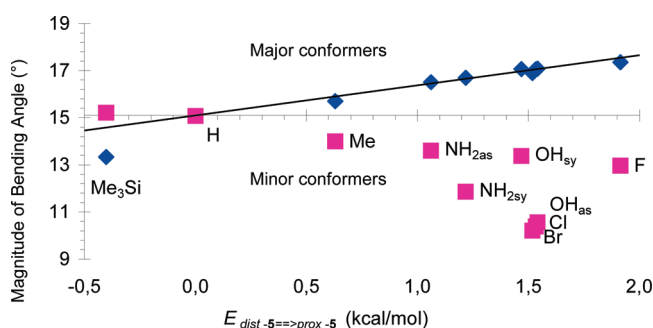


Figure 11. Magnitude of the bending angle in substituted carbenes **5** vs the difference in energy of both conformers.

($\Delta E_{\text{dist-5} \rightarrow \text{prox-5}}$) and the corresponding intramolecular TS (**5** \rightarrow **7**) (cf. Figure 12). This correlation is linear and has a slope slightly greater than unity. Assuming there is only one factor determining this line slope, two relationships are thus demonstrated: (1) the insertion ΔE^\ddagger is slightly affected by conformation, and (2) 1,3-CH insertion within the major conformers of **5** becomes a bit more facile as the *I* effect of R grows more withdrawing. This notion is reasonable considering that the major conformer is always bent to a higher degree than is the minor one and should be better poised for intramolecular 1,3-CH insertion (cf. Figure 13).

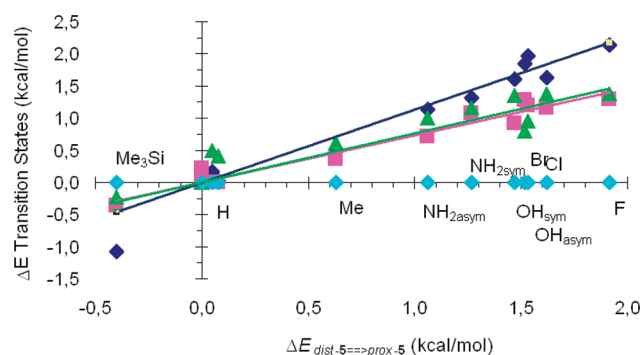


Figure 12. Correlation of the energy difference between carbene **5** conformers in the GS and at the pertinent TS (◆: intramolecular insertion; ■: insertion into CyH; ▲: formal insertion into MeOH).

The C-1–C-2–C-3 α -bridge of carbene **5** bends from the C-1–C-6–C-3 plane to stabilize **5**. The more the major conformer (cf. Figure 5) is bent toward (proximal; –) or away from (distal; +) the γ -substituent (R), the greater is the net energy difference between the conformers *prox-5* and *dist-5* ($\Delta E_{\text{dist-5} \rightarrow \text{prox-5}}$; cf. Table 2). Clearly, the magnitude of bending in the major conformer (*prox-5* with R_D and *dist-5* with R_A) is always greater than that in the minor one (*dist-5* with R_D and *prox-5* with R_A). This is because the extent of Cieplak- and Felkin–Anh-type MO interactions in **5** is greater with the major conformers than with the minor ones. In this study, the linear dependence of distal bending toward the reference face is of special interest, because *dist-5* is the major conformer for the several carbenes with an R_A (◆: distal bending toward the reference face; ■: proximal bending toward the substituted face).

The transition states for the formation of fluorodehydroadamantane **7h** represented in Figure 13 show that the incipient C-2–H and C-2–C- β bond lengths in (a) and (b), respectively, are essentially the same. Thus, regioselectivity must be determined before the TS. The relative importance of the Cieplak- and Felkin–Anh-type interactions is complicated. For *dist-5h*, 1,3-CH insertion of a C- β' –H bond takes place while the collinear C- α –C- β' bond (C-3–C-10) donates electron density to lp^* . This reduces the carbene's electrophilicity and perhaps its ability to insert. Note that the incipient C-2–C- β bond lengths are shorter (ca. 1.9 Å) than the incipient C-2–C bond length (ca. 2.4 Å)

calculated for the intermolecular C–H insertion of CyH (vide infra).

Table 6. NBO Electronic Parameters of the TS for 1,3-CH Intramolecular Insertion Reactions of Carbene **5h** Conformers

R	F	
carbene	<i>prox-5h</i>	<i>dist-5h</i>
lp (e^-) ^a	1.917	1.911
lp* (e^-) ^b	0.159	0.187
Product	<i>as-7h</i>	<i>s-7h</i>
Relative Yield (%)	8	92
TS(5h → 7h):		
$\sigma(\text{C–H})$ (e^-)	1.7069	1.7098
$\sigma^*(\text{C–H})$ (e^-)	0.1109	0.1086
lp (e^-) ^a	1.850	1.849
lp* (e^-) ^b	0.393	0.401
lp... $\sigma^*(\text{C–H})$ (kcal/mol)	22.9	22.7
lp*... $\sigma(\text{C–H})$ (kcal/mol)	116.3	113.3
Cieplak-type ΔE (kcal/mol)	34.00 ^c	33.72 ^c
	3.55 ^d	3.79 ^d
Felkin–Anh-type ΔE (kcal/mol)	5.37 ^e	5.55 ^e
	3.62 ^f	3.84 ^f

^aElectron occupancy of carbene **5h** HOMO or corresponding C atom in the TS. ^bElectron occupancy of carbene **5h** LUMO or corresponding C atom in the TS. ^cInteraction energy between lp^* and the C- α –C- β σ -BMO donor—C- α –C- β (C-3–C-4) for *prox-5h* and C- α –C- β' (C-3–C-10) for *dist-5h*—of the inserted C- β –H. ^dInteraction energy between lp^* and the C- α –C- β σ -BMO donor—C- α –C- β (C-1–C-9) for *prox-5h* and C- α –C- β' (C-1–C-8) for *dist-5h*—of the uninserted C- β –H. ^eInteraction energy between lp and the C- α –C- β σ^* -ABMO acceptor—C- α –C- β' (C-3–C-10) for *prox-5h* and C- α –C- β (C-3–C-4) for *dist-5h*—of the inserted C- β –H. ^fInteraction energy between lp and the C- α –C- β σ^* -ABMO acceptor—C- α –C- β' (C-1–C-8) for *prox-5h* and C- α –C- β (C-1–C-9) for *dist-5h*—of the uninserted C- β –H.

Table 6 lists the NBO electron populations of the lp and lp^* for both carbene **5h** conformers and their respective intramolecular 1,3-CH insertion TSs.⁴⁰ The analysis shows that lp^* occupancy ($\text{lp}^*_{\text{TS}} - \text{lp}^*_{\text{sh}}$) increases more than three times lp vacancy ($\text{lp}_{\text{TS}} - \text{lp}_{\text{sh}}$) upon going from the GS to the TS. This indicates that the ground-state carbene behaves as an electrophile and receives electron density from the C–H bond into

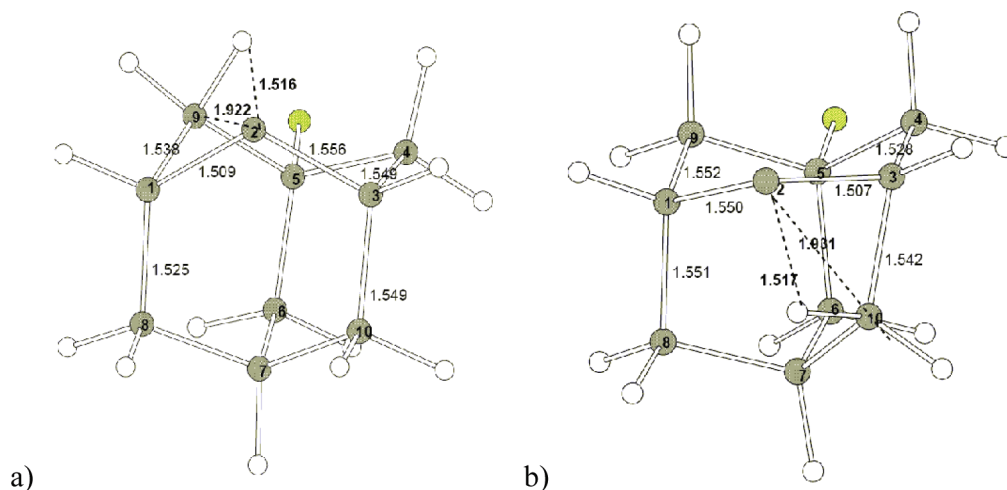


Figure 13. Representations of the **5h**-derived transition structures during intramolecular 1,3-CH insertion: (a) TS(*prox-5h* → *as-7h*) and (b) TS(*dist-5h* → *s-7h*). Distances in Å.

Table 7. Geometric Changes between the GS and TS of the Two Conformers of 5-Chloroadamantan-2-ylidene (*prox*- and *dist*-5g)

structure	$r(\text{C-2-H})$ (Å)	Δr (Å)	$r(\text{C-2-C-}\beta)$ (Å)	Δr (Å)
<i>prox</i> -5g	2.654	1.141	2.427	0.505
TS(<i>prox</i> -5g \rightarrow <i>as</i> -7g)	1.513		1.922	
<i>dist</i> -5g	2.578	1.062	2.369	0.439
TS(<i>dist</i> -5g \rightarrow <i>s</i> -7g)	1.516		1.930	

which it is inserting. This is highlighted by the development of a slightly negative charge on the divalent C atom, i.e., -0.08 NBO charge for TS(*dist*-5h \rightarrow *s*-7h). NBO analyses of carbenes *dist*- and *prox*-5h also give interaction energies between C- β -H and C-2 as a donor (lp) vs acceptor (lp*). The divalent C atom is a much better acceptor than donor (cf. Table 6). This finding also supports an electrophilic mechanism. Because the divalent C atom inserts into a C- β -H bond of C- α -C- β , the Cieplak- and Felkin-Anh-type interactions within the TS can be gauged. The Cieplak-type interaction of lp* with the C- α -C- β σ -BMO was remarkably high for the one with the C- β -H being inserted. This strong interaction is not nearly the case for the corresponding Felkin-Anh-type interaction.

The TS-geometry is not easily achieved for the minor isomer *as*-7g (cf. Table 7). The degree of bridge-bending again plays a crucial role. So, it is necessary to analyze the intramolecular distances closely. Table 7 shows that the major conformer *dist*-5g must change its relative geometry, i.e., C-2-H, by ca. 8% less than the minor conformer *prox*-5g. Carbenes *prox*- and *dist*-5g were used as an example, because carbene 5g has been closely investigated.²⁰

It is common to perform intermolecular carbene C-H insertion reactions using cyclohexane,⁴¹ because its carbon atoms are chemically equivalent; it simplifies product analysis. So, each 3H-diazirine 1 was dissolved in cyclohexane and photolyzed. As mentioned, up to 60% of 1 isomerizes to diazo compound 2 (Scheme 1). Because 2 does not react with aprotic cyclohexane, it has ample opportunity to couple with itself thereby forming substantial amounts of inert azine 3. Also, varying amounts of ketone 4 were observed, because the low-lying T₁ state becomes populated in the presence of trace amounts of oxygen. Notwithstanding, the cyclohexyl adducts 8 were obtained. They were configured in two diastereomeric forms, i.e., *syn*- and *anti*-8. The stereoselectivity clearly depends on R, as the relative ratios in Table 8 indicate.

Table 8. Ratios of Intermolecular C-H Insertion Products Obtained by the Photolysis of Aziadamantanes 1 in Cyclohexane

R	<i>syn</i> -8	<i>anti</i> -8	Ratio
Me ₃ Si	37	63	1:1.7
Me	67	33	2.0:1
NH ₂	79	21	3.8:1
OH	88	12	7.3:1
Br	87	13	6.7:1
Cl	89	11	8.1:1
F	92	8	11.5:1

Intermolecular insertion reactions of carbenes into C-H bonds differ from intramolecular ones in various ways. First, they have different molecularities. Intramolecular reactions are unimolecular, but intermolecular reactions are bimolecular and

may even be trimolecular in some cases (vide infra). In liquid-phase solution, both molecules must diffuse through the solvent to react. If they are inclined to do so then the reaction rate is limited only by viscosity. Indeed, the reaction rate may even exceed the diffusion limit, because carbene 5 reacts with the ubiquitous solvent itself. The activated complex at the TS is formed, however, by the collision of two particles into one and is expected to require a particular arrangement. Thus, the activation entropy is expected to be negative, i.e., $\Delta S^\ddagger < 0$ cal/(mol·K), thereby increasing ΔG^\ddagger (a,d) (cf. Figure 10). Nevertheless, reactive carbenes are known to undergo "barrierless" reactions wherein the entropic limitations are offset by negative activation enthalpies, i.e., $\Delta H^\ddagger < 0$ kcal/mol). This favorable attribute is not seen with intramolecular insertion reactions. Therefore, the more facile intermolecular C-H insertions are expected to be less selective than intramolecular ones.

Ab initio computations for the intermolecular insertion reactions of carbenes *prox*- and *dist*-5 with solvent suggest that product stereoselectivity is at least partially influenced by a nonzero $\Delta\Delta E^\ddagger$, as the insertion line slopes in Figure 12 indicate. But in contrast to intramolecular insertion, the less-than-unity line slopes mean that intermolecular insertions by the major conformers of 5 become a little less facile as the *I* effect of R grows stronger. This notion is reasonable considering that the major conformer is always bent to a higher degree than is the minor one. As can be shown by EFOE considerations (herein not listed), the reactive part of the LUMO is less accessible and should be less poised for intermolecular insertion. Regardless, the experimental isomer ratios for intra- (cf. Table 1) and intermolecular insertions (cf. Table 8 and Table 11, vide infra) are essentially the same. So, as with intramolecular bond insertion, intermolecular selectivity is dominated by the conformational ΔE rather than the insertion $\Delta\Delta E^\ddagger$ and is readily explained using the Curtin-Hammett principle (cf. Figure 10). Thus, the stereoselective formation of 8 (and 9, vide infra) also stems mainly from equilibrated carbene 5 conformers.

The insertion of a carbene into a C-H bond is considered to be concerted and electrophilic.⁴² So, the p-LUMO of the electron-deficient carbene may be envisioned approaching the target C atom and interacting with a filled C-H MO to form two new σ -bonds. The Bach model for intermolecular insertion of a carbene into a C-H bond posits two possible orientations at the TS: σ - and π -approach (cf. Figure 14).⁴³ A partial positive charge is supposed to develop on the solvent C atom.⁴⁴ And, as it approaches the TS, the divalent C atom in carbene 5b becomes more negatively charged, i.e., from $+0.14$ to -0.1 NBO charge. Therefore, the TS for intermolecular C-H bond insertion is somewhat polar. The kinetic barrier between the carbene reaction intermediate and the product depends on the net contributions of ΔH^\ddagger and ΔS^\ddagger . Again, the activation entropy is assumed to be negative, i.e., $\Delta S^\ddagger < 0$ cal/(mol·K),^{43,45} because the TS has a particular orientation. But this is expected to be offset by a negative activation enthalpy, i.e., $\Delta H^\ddagger < 0$ kcal/mol). Figure 15b shows the HOMO of the TS(5b \rightarrow 8b). The approach of carbene 5b toward cyclohexane is symmetric and it inserts preferably into an equatorial C-H bond, because this TS is 0.63 kcal/mol more stable than that for axial C-H insertion. An inspection of the HOMO of cyclohexane shows that it excludes the axial H atoms (cf. Figure 15a).⁴⁶

The activated complexes between each carbene 5a conformer and cyclohexane were also analyzed by the NBO method (cf. Figure 16a,b). The Cieplak- and Felkin-Anh-type interactions depicted in Figure 5 were quantified from the electron populations of lp, $\sigma(\text{C-H})$, lp*, and $\sigma^*(\text{C-H})$. At the TS,

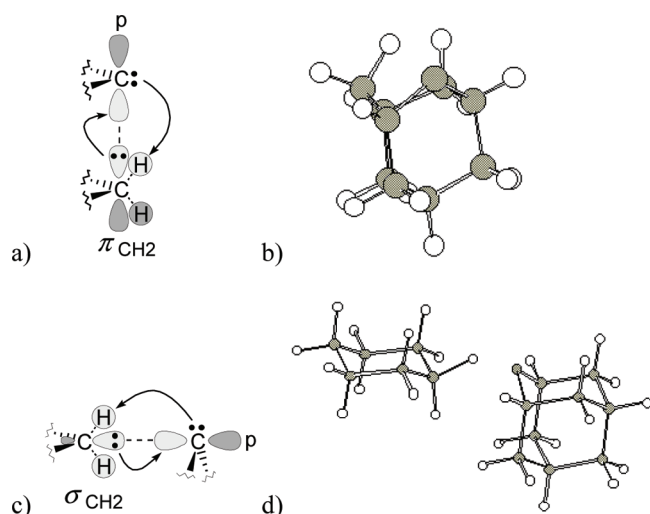


Figure 14. Frontier molecular orbital interaction of carbene C–H insertion into a methylene group depicting the (a) π_{CH_2} –p and (c) σ_{CH_2} –p approach. Overlap of the carbene's LUMO with the filled π_{CH_2} (b_1) group orbital is preferred for intramolecular insertion (b) and with the filled σ_{CH_2} (a_1) group orbital for intermolecular insertion (d).

the donor–acceptor $\text{lp} \cdots \sigma^*(\text{C}–\text{H})$ and acceptor–donor $\text{lp}^* \cdots \sigma(\text{C}–\text{H})$ interactions leading to C–H insertion are comparable in magnitude (cf. Table 9). Interaction between the carbene lp^* and the $\text{CyH} \sigma^*(\text{C}–\text{H})$ is possible, because the lp^* at C-2 is not empty. So, the $\text{lp}^* \cdots \sigma^*(\text{C}–\text{H})$ interaction was also analyzed (cf. Table 9). The major carbene **5** conformers were found to always have a later TS than the minor ones and be further advanced in the reaction. The results of the NBO analyses do support a concerted electrophilic mechanism for C–H insertion. This is made evident by the donor–acceptor interaction energies and the stretching of the inserted C–H bond. With an R_D , the divalent C atom in carbene **5** becomes less electron-deficient through electron donation. Though still electrophilic, the difference in $\text{lp} \cdots \sigma^*(\text{C}–\text{H})$ and $\text{lp}^* \cdots \sigma(\text{C}–\text{H})$ interactions is smaller than that with an R_A . Electron-donation to the $\sigma^*(\text{C}–\text{H})$ and from the $\sigma(\text{C}–\text{H})$ of cyclohexane is enhanced. Stabilization by the Felkin–Anh-type interaction is also augmented, because the TS leading to the main product is relatively tight, i.e., cyclohexane is close to the divalent C atom (cf. Figure 16a,b and Figure 14d). The interactions between each carbene FMO and the inserted C–H bond of cyclohexane were analyzed for the F-substituted carbenes *dist*- and *prox*-**5h** as well (cf. Figure 16d,e). The importance of Felkin–Anh-type stabilization increases if just the adamantanylidene moiety of the TS is considered, but the Cieplak-type stabilization is still greater. Although the magnitudes of the latter type are smaller than in ground-state carbenes **5** (cf. Table 3), the relative

Table 9. Structural and Electronic Parameters of the TS for the Intermolecular Reaction of Carbenes **5** and Cyclohexane

R	donor (R_D)		acceptor (R_A)	
	Me_3Si		F	
carbene	<i>prox</i> - 5a	<i>dist</i> - 5a	<i>prox</i> - 5h	<i>dist</i> - 5h
$\text{lp} (\text{e}^-)^a$			1.917	1.911
$\text{lp}^* (\text{e}^-)^b$	0.20	0.18	0.159	0.187
product	<i>anti</i> - 8a (major)	<i>syn</i> - 8a (minor)	<i>anti</i> - 8h (minor)	<i>syn</i> - 8h (major)
relative yield (%)	63	37	8	92
TS(5 \rightarrow 8):				
$\Delta r(\text{C}–\text{H})$ (Å)	1.294	1.288	1.250	1.261
$\sigma(\text{C}–\text{H}) (\text{e}^-)$	1.577	1.591	1.624	1.607
$\sigma^*(\text{C}–\text{H}) (\text{e}^-)$	0.249	0.240	0.205	0.214
$\text{lp} (\text{e}^-)^a$	1.70	1.71	1.74	1.73
$\text{lp}^* (\text{e}^-)^b$	0.54	0.53	0.49	0.51
$\text{lp} \cdots \sigma^*(\text{C}–\text{H})$ (kcal/mol)	136	131	95	99
$\text{lp}^* \cdots \sigma(\text{C}–\text{H})$ (kcal/mol)	153.8	144.52	125	136.22
$\text{lp}^* \cdots \sigma^*(\text{C}–\text{H})$ (kcal/mol)	47.3	44.9	37	40
Cieplak-type ΔE^c (kcal/mol)	9.65	9.47	9.71	9.95
Felkin–Anh-type ΔE^d (kcal/mol)	7.49	7.37	7.18	7.61

^aElectron occupancy of carbene **5** HOMO or corresponding C atom in the TS. ^bElectron occupancy of carbene **5** LUMO or corresponding C atom in the TS. ^cInteraction energies between lp^* and one of two C- α –C- β σ -BMO donors. These are C- α –C- β (C-1–C-9 and C-3–C-4) for *prox*-**5** and C- α –C- β' (C-1–C-8 and C-3–C-10) for *dist*-**5**. Note, the approach is symmetric. ^dInteraction energies between lp and one of two C- α –C- β σ^* -ABMO acceptors. These are C- α –C- β' (C-1–C-8 and C-3–C-10) for *prox*-**5** and C- α –C- β (C-1–C-9 and C-3–C-4) for *dist*-**5**. Note: the approach is symmetric.

importance between both types of stabilization differs only slightly from Me_3Si to F.

In addition to electron populations and interaction energies of selected orbitals in TS(*dist*-**5** \rightarrow *syn*-**8**) (cf. Figure 16), noticeable differences are found by comparing interatomic distances. The C- α –C- β and C- α –C- β' bonds at the TS become shorter, because of diminished electron-donation to the lp^* of the divalent C atom (cf. Table 10), when compared with those in ground-state carbenes **5**. Moreover, the bending angle of the carbene α -bridge at the TS is reduced (cf. Figure 7 and Figure 16). This lessens the distance between the divalent C atom and the inserted C–H bond. The major conformers benefit from this more than the minor ones, because the cyclohexane molecule approaches from the more exposed face. Thus, the *I* effects of R determine the preferred conformation

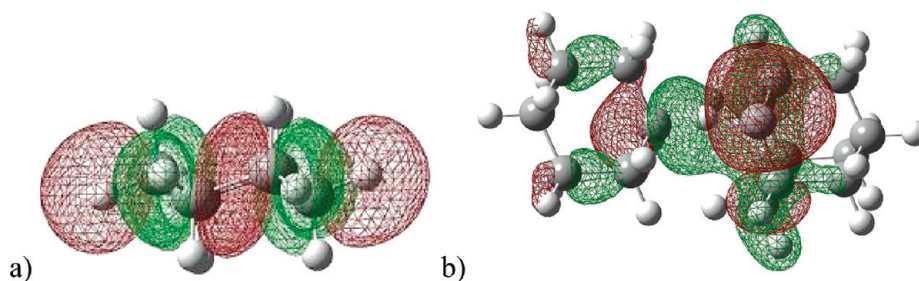


Figure 15. Contour plots for the insertion of carbene **5b** into CyH: (a) HOMO of CyH, (b) HOMO of TS(**5b** \rightarrow **8b**).

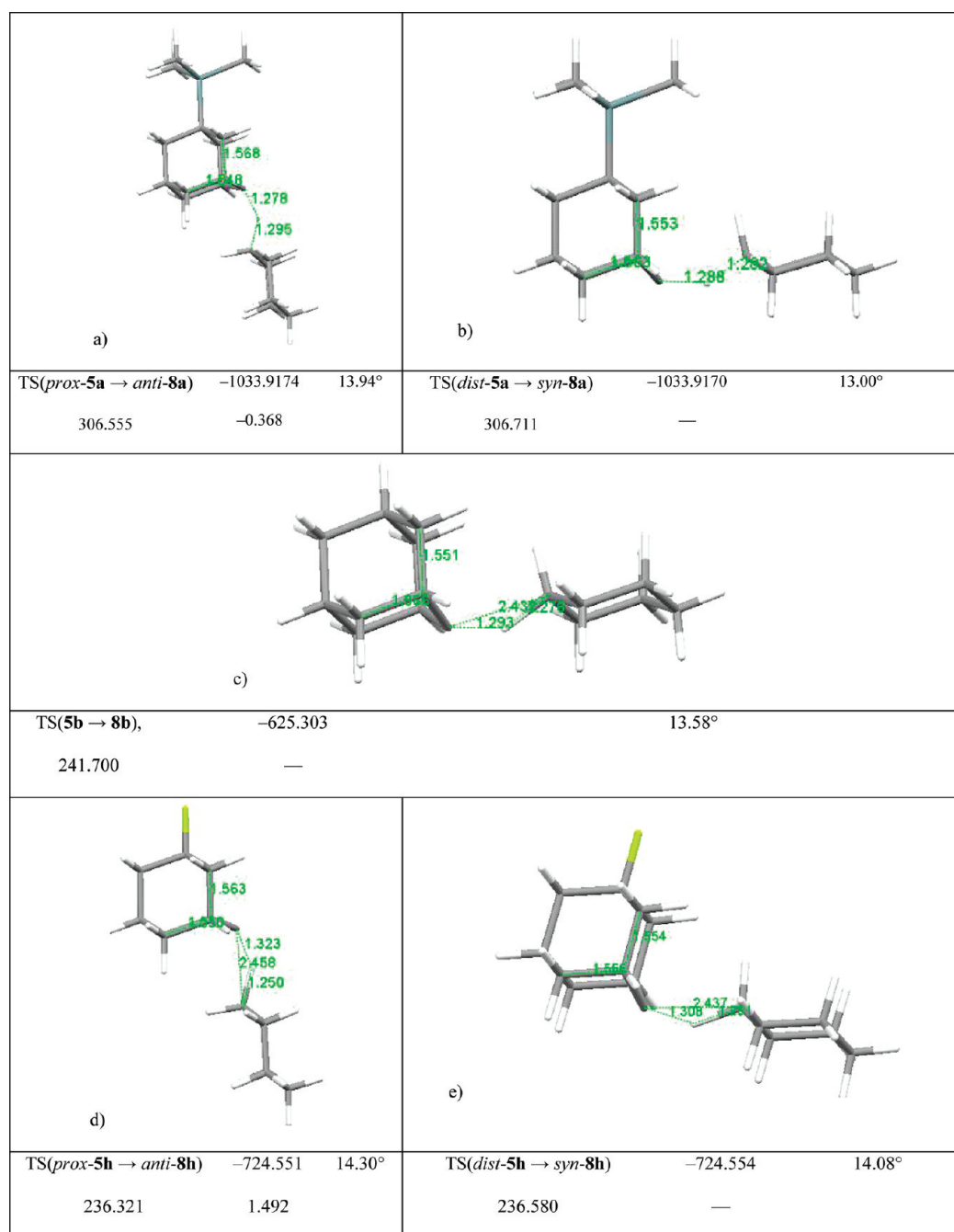


Figure 16. Structure and characteristics of the activated complex between carbenes **5** and cyclohexane: *E* (hartree), bending angle (deg), ZPVE (kcal/mol)) ΔE (kcal/mol; (–) exothermic vs (+) endothermic. Note: a and b were calculated at the B3LYP/6-31+G(d) level.

Table 10. Comparison of the Stabilizing Interactions in Carbene **5b and at the TS with Cyclohexane^a**

C- α -C- β bond	bond length (Å)	electron population	
		σ -BMO	σ^* -ABMO
5b:			
(C-3–C-4)	1.580	1.924	0.022
(C-3–C-10)	1.552	1.970	0.036
TS(5b \rightarrow 8b):			
(C-3–C-4)	1.565	1.943	0.0192
(C-3–C-10)	1.551	1.974	0.0347

^acf. Figure 16.

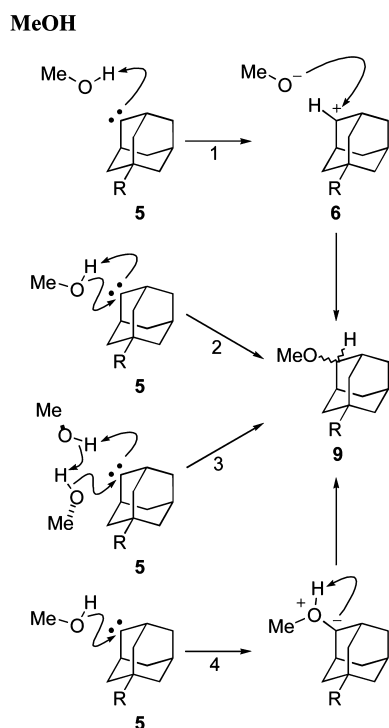
of **5** at the GS and they affect the reaction by controlling the degree of electron deficiency of the divalent C atom at the TS.

Photolysis of 3*H*-diazirines **1c–h** in MeOH mainly gave methyl ethers **9c–h**, which could be distinguished as either the *syn*- or *anti*-stereoisomer (cf. Table 11). It is clear that the relative amount of *syn*-**9** increases as the *I* effect of R increases.

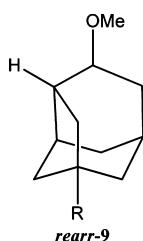
Complications arise when 3*H*-diazirine **1** is photolyzed in MeOH. As mentioned, up to 60% of **1** isomerizes to diazo compound **2** (Scheme 1). In aprotic media like cyclohexane, unstable **2** either expels N₂ and simply goes on to generate carbene **5** or it couples to give inert azine **3**. But in protic solvents, like water and alcohol, a diazo compound decays even faster, because it is readily protonated even by weak acids.⁴⁷ The resulting diazonium cation (not shown) releases N₂ and the ensuing cation **6** can also react with MeOH to yield **9**. So, isomeric product ratios may be skewed by dissimilar

Table 11. Ratios of Intermolecular O–H Insertion Products Obtained by the Photolysis of Aziadamantanes 1 in MeOH

R	with fumaronitrile			without fumaronitrile		
	<i>syn</i> -9	<i>anti</i> -9	ratio	<i>syn</i> -9	<i>anti</i> -9	ratio
Me ₃ Si	31	69	1:2.2	31	69	1:2.2
Me	64	36	1.8:1	60	40	1.5:1
NH ₂	81	19	4.3:1	73	27	2.7:1
OH	85	15	5.7:1	75	25	3.0:1
Br	83	17	4.9:1	77	23	3.3:1
Cl	85	15	5.7:1	79	21	3.8:1
F	91	9	10.1:1	84	16	5.3:1

Scheme 2. Proposed Mechanisms for the Formal Insertion of Carbene 5 into the O–H Bond of MeOH

selectivities of intermediates 5 and 6. Therefore, 2 must be rapidly trapped by dipolar addition with the efficient scavenger fumaronitrile (FN).^{24,48} Indeed, different product ratios were observed in its absence. And cation 6 left other clues. When 3*H*-diazirine 1b was photolyzed in methanol-*d*₄, typical amounts of 9b-*d*₄ (95%) and 7b-*d*₁ (5%) were formed. The absence of unlabeled 7b, however, rules out direct isomerization of carbene 5b. Exclusive label incorporation suggests another mechanism involving cation 6b or other suitable precursors of isotopomer 7b-*d*₁.⁴⁹ Another sign that route 2 → 6 is operative and must be thwarted by FN was formation of the skeletal



rearrangement product 7-substituted tricyclo[3.3.1.1^{2,7}]decan-3-yl methyl ether (*rearr*-9; 1.6%).⁵⁰

There is some ambiguity regarding the formal insertion of a carbene into an O–H bond.^{48,51} Several mechanisms for the intermolecular reaction of carbene 5 with MeOH are presented in Scheme 2: (1) a proton transfer followed by ion-pair recombination; (2) a concerted interaction between reactants; (3) a concerted trimolecular step with a “dimeric” reactant; and (4) oxonium ylide formation with subsequent Stevens rearrangement.⁵² Because it is not possible to assign an isomeric product ratio to each mechanism, other evidence is needed.

No C–H bond insertion by 5 was observed. This strict chemoselectivity of the reaction casts doubt on mechanism 2. It is further unlikely, because of the highly dipolar nature of the O–H bond and the strong influence of polarity on the TS.^{48a} In fact, the charge separation that arises in mechanisms 1 and 4 should be facilitated by a polar solvent, like MeOH (dielectric constant (κ) = 32.7). Further inspection of these pathways reveals that they are complementary; carbene 5 is an electrophile in mechanism 4, but it is a nucleophile in mechanism 1. Ostensibly, one might rule out mechanism 1 in favor of mechanism 4, because it seems unlikely that an electron-deficient carbene could act as an electron-donating nucleophile. However, there is growing evidence that this can occur. The simple FMO energies listed in Table 12 suggest that carbene 5b is at least ambiphilic.⁵³ So, if MeOH does oligomerize then the cyclic TS in mechanism 3 becomes quite plausible,⁵⁴ because electron-

Table 12. Comparison of the Energies of the Frontier Molecular Orbitals of Select Carbenes^a

carbene	E_{LUMO} (eV)	E_{HOMO} (eV)	π -bond reactivity
Cl–C–Cl	−3.75	−7.54	electrophilic
Me–C–Cl	−2.86	−6.50	electrophilic
MeO–C–Cl	−2.01	−6.94	ambiphilic
5b	−1.90	−5.09	ambiphilic
MeO–C–Me	−1.03	−5.71	nucleophilic
MeO–C–OMe	−0.49	−6.48	nucleophilic

^aB3LYP/6-31+G(d,p)//B3LYP/6-31+G(d) calculations.

donation from the O atom of one MeOH moiety enhances the nucleophilicity of the divalent carbon and induces proton transfer from the other. Here, the O–H insertion truly is formal, because the O and H atoms come from different molecules.

The propensity of carbene 5 to accept H⁺ from MeOH and form cation 6, as in mechanism 1, is a simple matter of acid–base chemistry. The gas-phase proton affinity (PA) of a carbene, which is the net energy required to protolyze its carbenium ion conjugate acid, is a thermodynamic quantity that parallels its Brønsted–Lowry basicity (K_b). This, in turn, often correlates with its nucleophilicity—a kinetic term. Although the K_b values for carbenes can be determined by comparison with those of known indicators, the PA values are usually calculated using theoretical methods, like *ab initio* B3LYP/6-31G(d).⁵⁵ Hence, the abilities of different carbenes to act as electron donors during an elementary step can be estimated and arranged. For example, the PA values of norbornanylidene and norbornenyldiene (254.7 and 263.0 kcal/mol, respectively) are higher than that of dichlorocarbene (209.0 kcal/mol), which suggests the former are nucleophiles that react with electrophiles, like H⁺, and the latter is an electrophile that reacts with nucleophiles, like π -rich alkenes. Indeed, the PA values for hydrocarbon carbenes can rival or even exceed those of the celebrated nucleophilic

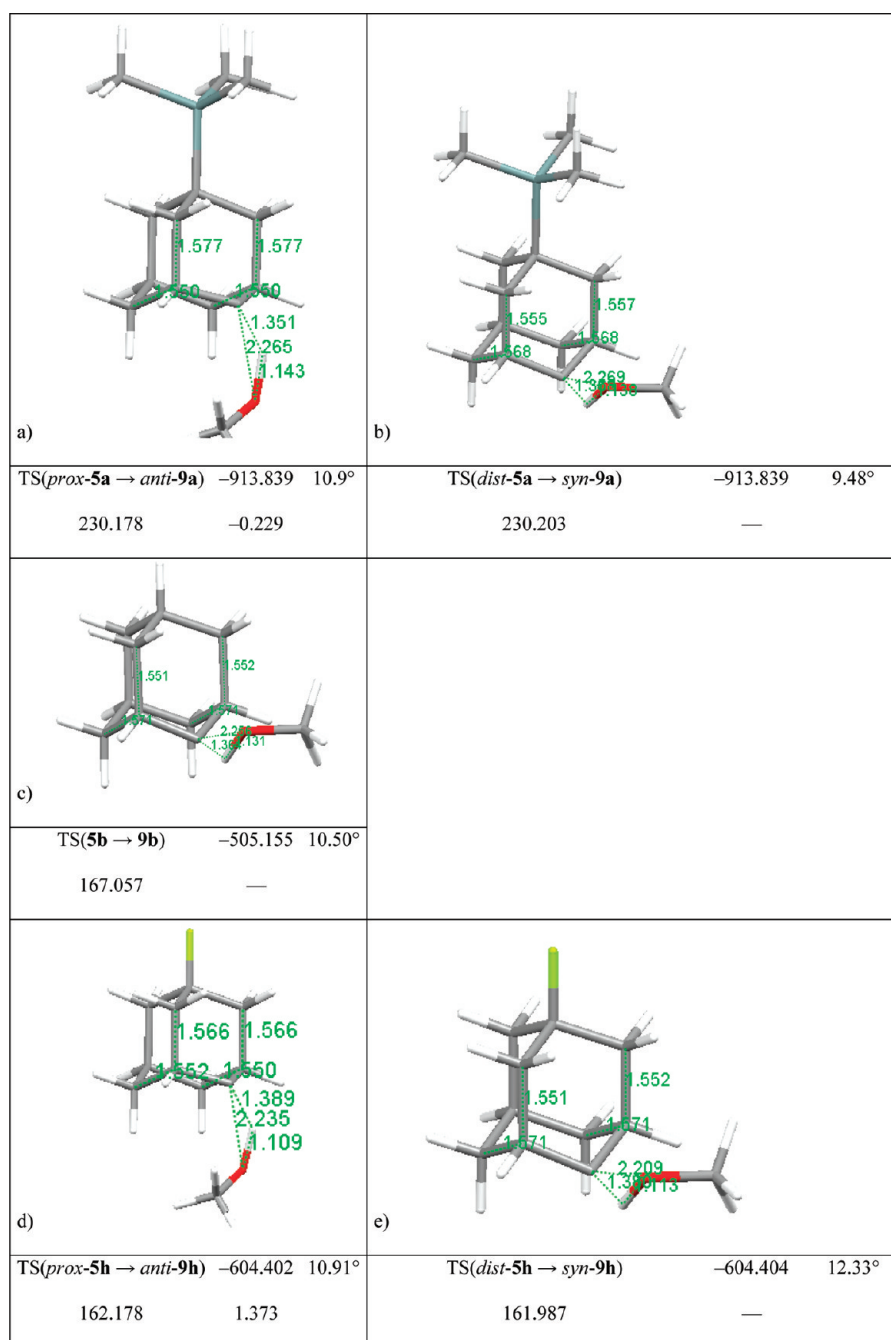


Figure 17. Structure and characteristics of the activated complex between carbenes **5** and MeOH: *E* (hartree), bending angle (deg), ZPVE (kcal/mol), ΔE (kcal/mol; (–) exothermic vs (+) endothermic).

carbenes imidazolylidene and 3,4-dimethylthiazolylidene (258.2 and 252.5 kcal/mol, respectively). And because the pK_a value of the latter's conjugate acid was estimated to be 16.5 in DMSO and 18.9 in H_2O ,⁵⁶ one may infer that 3,4-dimethylthiazolylidene and alkylcarbenes are readily protonated in relatively acidic hydroxylic solvents, like H_2O ($pK_a = 15.7$) and MeOH ($pK_a = 15.5$). So, the participation of carbene **5** in mechanism 1 deserves further consideration, because the calculated PA value of **5b** (268.9 kcal/mol; B3LYP/6-31G(d)) is even higher than that of norbornenyldiene. Its greater basicity and nucleophilicity, which is also supported by FMO analysis, likely comes from the absence of ring strain in carbenes **5**. Finally, if cation **6** can rearrange faster than it recombines with its counterion then observing products stemming from **6** is another way to support mechanism 1. Of

course, one would need to exclude all other channels leading to cation **6**, e.g., **2** → **6**.

Now, even if protonation of carbene **5** by an O–H group is an energetically favored step, it could be a kinetically stymied one. In addition to basicity, other factors that determine nucleophilicity, like charge and polarizability, may need to be considered. It is conceivable that **5** reacts with MeOH to form a methoxonium ylide, as in mechanism 4. Such routes are widely supported, because the formation of ylides from electrophilic carbenes has been directly observed.⁵⁷ However, neutral O atoms are not strong nucleophiles and the ability of Et_2O and MeOH to form oxonium ylides is weak.⁵⁸ Thus, it seemed most worthwhile to explore mechanism 1.

Table 13. Structural and Electronic Parameters of the TS for the Intermolecular Reaction of Carbene **5h** and MeOH

R	acceptor (R _A)	
	F	
carbene	<i>prox-5h</i>	<i>dist-5h</i>
lp (e ⁻) ^a	1.917	1.911
lp* (e ⁻) ^b	0.159	0.187
product	<i>anti-9h</i> (minor)	<i>syn-9h</i> (major)
relative yield (%)	9	91
TS(5 → 9):		
Δr(O–H) (Å)	1.11	1.13
σ(O–H) (e ⁻)	1.833	1.822
σ*(O–H) (e ⁻)	0.267	0.27
lp (e ⁻) ^a	1.706	1.702
lp* (e ⁻) ^b	0.363	0.385
lp...σ*(O–H) (kcal/mol)	123.2	123.8
lp*...σ(O–H) (kcal/mol)	39.0	43.55
lp*...σ*(O–H) (kcal/mol)	9.33	10.32
Cieplak-type ΔE (kcal/mol) ^c	9.91, 10.11	11.43, 11.28
Felkin–Anh-type ΔE (kcal/mol) ^d	5.12, 5.21	5.78, 5.9

^aElectron occupancy of carbene **5** HOMO or corresponding C atom in the TS. ^bElectron occupancy of carbene **5** LUMO or corresponding C atom in the TS. ^cInteraction energies between lp* and both C-α-C-β σ-BMO donors are given. These are C-α-C-β (C-1–C-9 and C-3–C-4) for *prox-5* and C-α-C-β' (C-1–C-8 and C-3–C-10) for *dist-5*. Note, the approach is not symmetric. ^dInteraction energies between lp and both C-α-C-β σ*-ABMO acceptors are given. These are C-α-C-β' (C-1–C-8 and C-3–C-10) for *prox-5* and C-α-C-β (C-1–C-9 and C-3–C-4) for *dist-5*. Note, the approach is not symmetric.

Although the reaction kinetics of transient carbene **5b** with cyclohexane are fast ($t_{1/2} = 20$ ns; pseudo-first-order rate constant $k_{\text{obs}} < 5 \times 10^7 \text{ s}^{-1}$),^{36a} the measurement of those for “invisible” S₀ carbene **5** with MeOH are limited only by indicator diffusion.^{24b,59} The reaction of carbene **5** with MeOH is almost instantaneous. So, if protonation mechanism 1 is operative then it is not hampered at all. The TS of the insertion of carbene **5** into MeOH is computed to indeed be 6.3 kcal/mol more stable than the isolated reactants.⁶⁰ Therefore, here is another example of a “barrierless” reaction with $\Delta S^\ddagger < 0 \text{ cal/(mol·K)}$ and $\Delta H^\ddagger < 0 \text{ kcal/mol}$ (vide supra).

As discussed,^{4b,11} the protonation of carbene **5b** is predicted to be favored both thermodynamically and kinetically. Indeed, protonation of carbenes **5** might be a straightforward way to generate “free” 2-adamantanylium cations **6**, whose reactions in MeOH have been well examined.^{4a,11} Regardless, protonation mechanism 1 is fundamentally different from the others outlined in Scheme 2, because nucleophilic behavior of a carbene is unconventional. A proton would interact first with the HOMO of **5**. But the stabilizing Cieplak- and Felkin–Anh-type interactions in the resulting cation **6** should mimic those in the isoelectronic carbene **5**. Indeed, the $\Delta E_{\text{dist} \rightarrow \text{prox}}$ values between their respective conformers are similar and structural response to the *I* effect of R appears to be the same for both intermediates **5** and **6**. So, similar stereoselectivities might be expected if it were not for the fact that the activation energies for **5** → **9** and **6** → **9** are different. The computed $\Delta\Delta E^\ddagger$ values, however, have been found herein to be minimal and that product stereoselectivity is based mainly on the $\Delta E_{\text{dist} \rightarrow \text{prox}}$ between the conformers (cf. Figure 10). Thus, if protonation of **5** does occur then it is likely to have only a small effect on the isomeric product ratios.

Table 14. Distances between the Divalent Carbon (C-2) and the O–H Bond of MeOH at the TS for Intermolecular O–H Insertion

activated complex	<i>r</i> (C-2–O) (Å)	<i>r</i> (C-2–H) (Å)
TS(<i>dist-5a</i> → <i>syn-9a</i>)	2.269	1.358
TS(5b → 9b)	2.256	1.364
TS(<i>dist-5h</i> → <i>syn-9h</i>)	2.209	1.380

NBO analyses were performed on the methanolysis TS of the following carbenes: *dist*- and *prox-5a*, *dist*- and *prox-5c*, *dist*- and *prox-5h*, and parent carbene **5b**. They predict that MeOH approaches from the more exposed face of carbene **5** (cf. Figure 17). This means that *anti-9a* will predominate, because carbene **5a** spends more time in its proximal conformation. Although the TS(**5h** → **9h**) was found to be earlier than the others, likewise predictions were made. Because *dist-5h* outnumbers *prox-5h*, *syn-9h* is expected to abound. The inversion in diastereoselectivity reflects the different *I* effects of R, which reverse from an R_D to an R_A. It is not unreasonable that a nucleophilic carbene would be attracted to the protic H atom of MeOH, because it bears a sizable partial positive charge (+0.45).⁶¹

Indeed, NBO analysis found that the donor–acceptor lp...σ*(O–H) interaction between carbene **5** and MeOH at the TS was much greater than the acceptor–donor lp*...σ(C–H) interaction leading to O–H insertion (cf. Table 13). Therefore, unlike electrophilic insertion of **5** into the C–H bond of CyH (cf. Table 9), formal insertion into the O–H bond of MeOH is made by a nucleophilic carbene **5**. As with cyclohexane, there is an interaction between both “vacant” orbitals. Because electron-density was donated into the lp*, it is not empty and interaction between the carbene **5** lp* and the MeOH σ*(O–H) is possible. So, the lp*...σ*(O–H) interaction was analyzed as well (cf. Table 13). Evaluation of the Cieplak- and Felkin–Anh-type interactions gave typical values. As with cyclohexane (cf. Table 9), the Cieplak-type were stronger. The major carbene conformer is more stabilized by these interactions than is the minor one. The conclusion is that the carbene insertion into MeOH is nucleophilic and involves a protic mechanism.⁶² Compared with the more electron-rich carbenes **5a** and **5b**, the distance between C-2 and the O atom of MeOH for carbene **5h** is shorter at the TS (cf. Table 14). In contrast to the unsubstituted carbene **5b**, the electron-deficient carbenes *dist*- and *prox-5h* prefer the approach of the O atom's lone-pair of electrons, i.e., mechanism 4, slightly more than protonation, i.e., mechanism 1. Regardless, the distance between the divalent C atom and the O atom seems long (2.256 Å). One should keep in mind, however, that these are gas-phase calculations with inherent disadvantages. We will show only the results for compound **9h** where the NBO analysis of the TS did not attribute the H atom to the divalent carbon in **5** anymore, because of the reasons listed in note 61.

The protonation of carbenes **5** and resulting formation of cations **6** cannot be excluded. But one ensures that the presence of cations **6** is due only to the protonation of carbene **5** by capturing diazo compounds **2** before their protonation. Unfortunately, it is not possible to differentiate between reaction intermediates **5** and **6** based solely on product diastereoselectivities, because they differ only slightly (cf. Figure 3).^{4b} This might be expected, because the ΔE values for the rapid equilibrium between *prox*- and *dist-6* are similar to those for the corresponding carbene **5** conformers.⁶³ A comparison of carbene **5a** and cation **6a** presents an interesting counter-

example, however, because the observed isomeric product ratios and computed ΔE values^{11,63} differ significantly. Nevertheless, product selectivities are usually correlated with the I effect of R^{64a} . Thus, the insertion product ratios may be predicted from the GS of the reaction intermediates alone and Cieplak's model of electron-donation into the σ^* -ABMO of the incipient bond during the TS is not needed.

CONCLUSION

3*H*-Diazirines **1** are labile compounds that generate carbene **5** reaction intermediates when exposed to heat or light. The α -bridges of the reaction intermediates bend to maximize the stabilizing effects of Cieplak- and Felkin-Anh-type orbital interactions, which are atypically *cooperative* here. Because the transients have substituted and unsubstituted faces, this leads to proximal and distal conformational isomers that are in rapid equilibrium with each other. The energy and relative population of each conformer depends on the σ -bond inductive effect of the γ -substituent. The proximal conformer is favored when it is an electron-donor and the distal one when it is an electron-acceptor. Each conformer leads to a unique TS and the ratio of isomeric products reflects the ratio of carbene conformers.

Selectivity is observed for both intra- and intermolecular insertion reactions. The warped structure of each carbene conformer is responsible for the reciprocity between intramolecular regioselectivity and intermolecular stereoselectivity. Because the proximal carbene is the major conformer when the γ -substituent is an electron-donor, it is simultaneously poised to favorably produce the *as*- and *anti*-products. The C–H bond of the former is already within reach of the bent carbene, whose exposed reference face is more apt to receive an incoming solvent molecule. And because the distal carbene is the major conformer when the γ -substituent is an electron-acceptor, it is ready to proliferate the *s*- and *syn*-products. Again, the C–H bond of the former is already within reach of the bent carbene, whose exposed substituted face is more receptive to an incoming solvent molecule.

Photolysis of 3*H*-diazirines **1** produces a substantial amount of diazo compounds **2**, which may also be a source of carbenes **5**. This appears to be unlikely, however, because their coupling was probably responsible for the extensive formation of inert azines **3** in aprotic CyH. In protic MeOH, the diazo compounds were protonated faster than they could couple and no azines **3** were formed. This side reaction had the potential of producing cations **6**, which were not under investigation. So, the potent dipolarophile fumaronitrile was used to capture dipolar **2** and permit the isomeric product ratios to be attributed to carbene **5** alone. This does not preclude **5** from being protonated to form **6**, because the electron-deficient carbene is predicted to behave as a nucleophile in hydroxylic solvents.

The differences in energy between proximal and distal carbenes **5** decrease toward the intermolecular TS.^{64b} This implies that neither TS stabilization nor a TS model is necessary to explain carbene **5** selectivity. Ground-state hyperconjugation alone is sufficient to explain the observed ratios, although this might be different for a late TS.¹⁰ For the cases studied here, this is a natural consequence of the reaction and increased interaction with the solvent and therefore the reduced steering influence of the substituent within the adamantanylidene moiety. It should be emphasized that both the Cieplak- and Felkin-Anh-type stabilizations favor the same conformer, but the Felkin-Anh type has less relevance for γ -substituted

adamantanylidenes. Similar conclusions could be made for γ -substituted 2-adamantylum cations.¹¹

COMPUTATIONAL METHODS

Density functional theory (DFT) *ab initio* MO calculations were performed using the Gaussian 03 program.⁶⁵ The hybrid method used combines Becke's three-parameter exchange functional with the correlation functional of Lee, Yang, and Parr (B3LYP).⁶⁶ Unless otherwise stated, the B3LYP method^{66,67} was used with a 6-31G(d) basis set for geometry optimizations and a larger 6-31+G(d,p) basis set for single-point energies. Vibrational frequency analyses were performed on each stationary point within energy minima, in order to make zero-point vibrational energy (ZPVE) corrections. The values discussed in the text represent internal energies (E) at 0 K. Quantification of donor–acceptor interactions was made by second-order perturbation analysis as incorporated in the natural bond orbital (NBO) method.

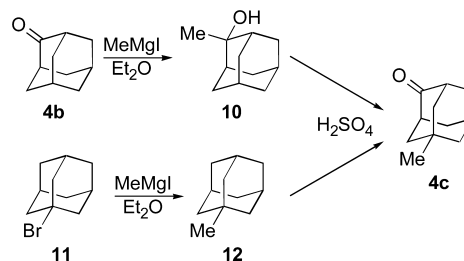
EXPERIMENTAL SECTION

General Information. FT NMR spectra were recorded at $T = 300$ K on spectrometers at the following Larmor frequencies: $\omega_L(^1\text{H}) = 250.1$, 400.13, and 600.13 MHz, respectively, and $\omega_L(^{13}\text{C}) = 62.9$, 100.58, and 150.86 MHz, respectively. Although δ_H and δ_C values for chemical shifts were measured relative to tetramethylsilane (TMS), the deuterated solvents were not doped with TMS but rather their residual peaks were used to calibrate the ^1H and ^{13}C NMR spectra, e.g., $\delta_H(\text{CHCl}_3) = 7.24$ ppm and $\delta_C(\text{CDCl}_3) = 77.02$ ppm. Coupling constants (J) are reported in Hz. Structural assignments are made on the basis of 2-D COSY, NOESY, HMQC, and HMBC. IR absorption spectra were recorded on a FT IR spectrometer using KBr pellets, except otherwise noted. UV/vis absorption spectra were measured on a double-beam spectrometer. Melting points were measured on a Kofler-type melting point microscope and are uncorrected. Photolyses were conducted using a 700-W medium pressure Hg-arc lamp doped with FeI_2 and equipped with a Pyrex filter. Electron impact (EI) spectra were obtained at 70 eV. Preparative GC was performed using an instrument equipped with SE-30 or Carbowax/KOH glass columns. Tandem GC-MS analyses were conducted on an instrument outfitted with a column and a mass selective detector (70 eV) using helium as carrier gas. Analytical gas chromatograms were obtained on a GC instrument equipped with a flame-ionization detector and a capillary column in order to determine product ratios, when applicable.

Preparation and Reactions of 3*H*-Diazirines. Ketone derivatives **4** were usually synthesized from 5-hydroxyadamantan-2-one (**4e**), but 5-methyladamantan-2-one (**4c**) was obtained in concentrated H_2SO_4 either by isomerization of 2-methyladamantan-2-ol (**10**) or by oxidation of methyladamantane (**12**) (Scheme 3).⁶⁸

These syntheses are well described and are to be found in the literature. The yields of the oxidation were 12% for the first and 7% for

Scheme 3. Syntheses of 5-Methyladamantan-2-one (**4c**)



the lower pathway. Note, however, that the upper pathway affords the cleaner product, because byproducts are not easily removed in the second pathway.

Via 2-methyl-2-adamantanol (10**):**^{68g} δ_H /ppm (2501 MHz, CDCl_3) 1.30 (CH_3), 1.53 (2 H, d J 4.5), 1.55 (1 H), 1.65–2 (10 H,

m), 2.2 (2 H, d J 12.26); $\delta_{\text{C}}/\text{ppm}$ (62.9 MHz, CDCl_3) 27.0, 27.4, 27.52, 32.9, 35.1, 38.3, 39.1, 73.8; m/z (EI) 166 (0.08), 152 (10), 151 (100), 148 (11), 133 (6).

1-Methyladamantane (12): m/z (EI) 150 (14), 136 (10), 135 (100), 107 (6), 93 (20), 79 (11).

5-Methyladamantan-2-one (4c): mp 117–119 °C; $\delta_{\text{H}}/\text{ppm}$ (250.1 MHz, CDCl_3) 0.92 (3 H, s), 1.7–1.82 (6 H, m), 1.95–2.01 (4 H, m), 2.1–2.16 (1 H, m), 2.53 (2 H, s); $\delta_{\text{C}}/\text{ppm}$ (62.9 MHz, CDCl_3) 28.1, 29.2, 30.0, 38.6, 43.4, 45.6, 46.6 (C=O was not recorded); m/z (EI) (13.16 min): 165 (12), 164 (100), 131 (20), 118 (12), 107 (12), 106 (16), 95 (17), 94 (20), 93 (76), 92 (20), 91 (20), 80 (14), 79 (29).

The general synthesis of 3H-diazirines from their corresponding ketones is well documented.²⁹ The syntheses of γ -substituted azadamantanes **1a**, **1d**, **1e**, **1f**, **1g**, and **1h** are reported elsewhere.^{24,69} The reactions with hydroxylamine-O-sulfonic acid (HOSA) in methanolic ammonia were performed at $T = -15$ °C. The putative diaziridines were not isolated, but directly oxidized. Compounds **1e**, **1f**, **1g**, and **1h** are described elsewhere. Likewise, data for the MeOH-insertion products from carbenes **5a**, **5c**, **5e**, and **5h**,^{16a} as well as some of the intramolecular insertion products may be found elsewhere.^{20,23} All data, except for **1h** and derivatives of **1e**, are listed in the Supporting Information. Photolyses were performed in anhydrous cyclohexane or anhydrous MeOH. Argon gas was bubbled through the solutions for 10 min, and the diazirines were photolyzed for 2.5 h at $T = 12$ –14 °C. The mixtures were analyzed by analytical GC and afterward separated or purified either by liquid-chromatography or by preparative GC (vide infra).

Gas-Phase Pyrolysis Experiments. The gas-phase pyrolysis experiments were performed either in a classical manner (method 1) or in the injector unit ($T = 270$ °C) of a preparative GC (method 2).

Method 1. A three-necked 100-mL round-bottom flask equipped with a twistable solids addition flask, a stopper, and a trap immersed in an ice–water bath was evacuated to 0.5 Torr. The solids addition flask was charged with the diazirine and the round-bottom flask was heated to $T = 250$ –300 °C. The solid diazirine was slowly released from the solids addition flask onto the heated surface of the round-bottom flask in small portions. The products from the decomposition were collected in a trap and in the glass tube connecting the trap with the round-bottom flask.

Method 2. An aliquot containing 40 mg of diazirine in 80 μL of CHCl_3 was slowly injected into the injector unit (column 15% SE-30 at 180 °C, gas flow at 80 mL/min). Working on a preparative GC can cause a substantial loss of substance for two reasons: (1) the volatility of the formed adamantane derivatives and (2) the suspected formation of azine in the injector block. When using a lower gas flow and a lower column temperature, the number of byproducts increased. With the exception of compounds *s*- and *as*-**7a** and *s*- and *as*-**7d**, pyrolytic insertion products could not be separated.

The azines were synthesized as reference compounds with the following method: 0.11 mmol of the corresponding diazirine was photolyzed in a rotating flask cooled to 5 °C for 2 h. The crude product was dissolved in chloroform and analyzed by GC and GC–MS. For the NMR analyses the crude product was washed with hot petroleum ether and dried in vacuo.

Preparation and Reactions of 4-Azi-1-(trimethylsilyl)-adamantane (1a).^{21b} The synthesis of 3H-diazirine **1a**, as described elsewhere,^{21b} was achieved in a yield of 43%: mp 38–39.5 °C; $\delta_{\text{H}}/\text{ppm}$ (250.1 MHz, CDCl_3) –0.04 (9 H, s), 0.64 (2 H, s), 1.60–1.71 (4 H, m), 1.74 (2 H, d J 11), 1.92–2.15 (5 H, m); $\delta_{\text{C}}/\text{ppm}$ (62.9 MHz, CDCl_3) –5.4 (–Si(CH₃)₃), 20.9 (C-1), 27.1 (C-7), 34.1 (C-3/C-5), 35.0 (C-2/C-9), 35.2 (C-6/C-10), 36.4 (C-8), (C-4 not obsd); $\bar{\nu}_{\text{max}}/\text{cm}^{-1}$ (KBr) 2921, 2849, 1571, 1450, 1243, 1132, 1080, 1056, 997, 950, 866, 831; $\lambda_{\text{max}}/\text{nm}$ (C₆H₁₂) 356 ($\epsilon/(10^4 \text{ M}^{-1}\text{cm}^{-1})$ 0.17), 362 ($\epsilon/(10^4 \text{ M}^{-1}\text{cm}^{-1})$ 0.14), 376 ($\epsilon/(10^4 \text{ M}^{-1}\text{cm}^{-1})$ 0.23); m/z (EI) 219 ([M – CH₃]⁺, 0.6%), 206 ([M – N₂]⁺, 2), 132 (9), 91 (9), 74 (9), 73 (100); found [M – CH₃]⁺ 219.1319, C₁₂H₁₉N₂Si requires 219.1318). Anal. Calcd for C₁₃H₂₂N₂Si: C, 66.61; H, 9.46; N, 11.95. Found: C, 66.92; H, 9.59; N, 12.14.

2,4-Didehydro-1-(trimethylsilyl)adamantane (as-7a): The pyrolysis of 3H-diazirine **1a** yielded intramolecular insertion products *s*-**7a** (4%) and *as*-**7a** (10%) (isolated ratio = 26:74). The separation was performed by preparative GC ($T_{\text{oven}} = 140$ °C, $T_{\text{injector}} = 260$ °C).^{21b} $\delta_{\text{H}}/\text{ppm}$ (250.1 MHz, CDCl_3) –0.02 (9 H, s), 1.19–1.29 (2 H, m), 1.31–1.37 (3 H, m), 1.41–1.45 (2 H, m), 1.47–1.51 (1 H, m), 1.80–1.88 (3 H, m), 2.00–2.10 (1 H, m), 2.34–2.36 (1 H, m); $\delta_{\text{C}}/\text{ppm}$ (62.9 MHz, CDCl_3) –4.2 (–Si(CH₃)₃), 21.4 (C-3), 25.3 (C-4), 25.6 (C-2), 26.8 (C-7), 27.7 (C-1), 28.7 (C-10), 33.1 (C-5), 33.3 (C-6), 33.6 (C-8), 53.6 (C-9); $\bar{\nu}_{\text{max}}/\text{cm}^{-1}$ (CCl₄) 3022, 3003, 2954, 2915, 2850, 1453, 1441, 1247, 1056, 1043, 930, 891, 869, 858, 848, 685; m/z (EI) 208 ([³⁰Si]M and [²⁹Si]M + H]⁺, 7%), 207 ([²⁹Si]M and M + H]⁺, 28), 206 (M⁺, 100), 191 (39), 132 (47), 117 (11), 92 (20), 91 (21), 79 (18), 74 (33), 73 (85); found M⁺ 206.1492, C₁₃H₂₂Si requires 206.1491.

2,4-Didehydro-7-(trimethylsilyl)adamantane (s-7a): $\delta_{\text{H}}/\text{ppm}$ (250.1 MHz, CDCl_3) –0.10 (9 H, s), 1.15–1.25 (1 H, m), 1.28–1.32 (4 H, m), 1.38 (1 H, dm J 9.5), 1.45–1.50 (2 H, m), 1.70–1.77 (2 H, m), 2.06–2.16 (1 H, m), 2.18–2.27 (2 H, m); $\delta_{\text{C}}/\text{ppm}$ (62.9 MHz, CDCl_3) –5.7 (–Si(CH₃)₃), 18.0 (C-7), 19.5 (C-3), 23.5 (C-2/C-4), 28.1 (C-10), 31.2 (C-1/C-5), 32.8 (C-6/C-8), 52.4 (C-9); $\bar{\nu}_{\text{max}}/\text{cm}^{-1}$ (CCl₄) 3026, 2988, 2954, 2923, 2846, 1247, 934, 875, 858, 846; m/z (EI) 207 ([³⁰Si]M and M + H]⁺, 5%), 206 (M⁺, 25), 79 (27), 73 (100); found M⁺ 206.1488, C₁₃H₂₂Si requires 206.1491.

anti-4-Cyclohexyl-1-(trimethylsilyl)adamantane (anti-8a): Photolysis of 3H-diazirine **1a** in CyH afforded a mixture of *syn*- and *anti*-4-cyclohexyl-1-(trimethylsilyl)adamantane *syn*-**8a**/*anti*-**8a** (ratio = 38:62) in 64% yield. In addition, 18% of azines **3a** were formed. The insertion products were separated by preparative GC on a 15% SE-30 column ($T_{\text{oven}} = 250$ °C, $T_{\text{injector}} = 220$ °C): mp 86.5–88.5 °C; $\delta_{\text{H}}/\text{ppm}$ (600.13 MHz, C₆D₆)⁷⁰ 0.08 (9 H, s), 0.88–0.90 (2 H, m), 1.25–1.45 (4 H, m), 1.57 (2 H, d J 12.5), 1.60–1.66 (1 H, m), 1.68 (2 H, d J 12), 1.74 (2 H, s), 1.78–1.83 (1 H, m), 1.84–1.90 (5 H, m), 1.93–2.01 (4 H, m), 2.03 (2 H, s); $\delta_{\text{C}}/\text{ppm}$ (150.9 MHz, C₆D₆)⁷¹ –5.6 (–Si(CH₃)₃), 20.9 (C-1), 26.8 (C-3'/C-5'), 27.0 (C-4'), 27.5 (C-7), 28.1 (C-3/C-5), 30.8 (C-2'/C-6'), 32.0 (C-6/C-10), 36.6 (C-1'), 37.9 (C-8), 39.1 (C-2/C-9), 49.7 (C-4); $\bar{\nu}_{\text{max}}/\text{cm}^{-1}$ (KBr) 2920, 2850, 1632, 1445, 1342, 1316, 1255, 1240, 941, 867, 832, 741, 684, 623; m/z (EI) 292 ([³⁰Si]M and [²⁹Si]M + H]⁺, 6%), 291 ([²⁹Si]M and M + H]⁺, 24), 290 (M⁺, 100), 217 (15), 165 (25), 162 (57), 149 (11), 135 (11), 79 (14), 73 (86); found M⁺ 290.2434, C₁₉H₃₄Si requires 290.2430. Anal. Calcd for C₁₉H₃₄Si: C, 78.54; H, 11.79. Found: C, 78.60; H, 11.48.

syn-4-Cyclohexyl-1-(trimethylsilyl)adamantane (syn-8a): mp 83.5–85.0 °C; $\delta_{\text{H}}/\text{ppm}$ (250.1 MHz, C₆D₆)⁷⁰ 0.07 (9 H, s), 0.80–1.02 (2 H, d J 13), 1.25–1.35 (4 H, m), 1.4–1.5 (2 H, d J 14), 1.55–1.70 (1 H, m), 1.74 (2 H, s), 1.81–2.13 (14 H, m); $\delta_{\text{C}}/\text{ppm}$ (62.9 MHz, C₆D₆)⁷¹ –5.5 (–Si(CH₃)₃), 20.6 (C-1), 26.9 (C-3'/C-5'), 27.1 (C-4'), 28.0 (C-7), 28.3 (C-3/C-5), 31.1 (C-2/C-9), 31.6 (C-2'/C-6'), 36.9 (C-1'), 38.1 (C-8), 39.7 (C-6/C-10), 49.8 (C-4); $\bar{\nu}_{\text{max}}/\text{cm}^{-1}$ (KBr) 2932, 2902, 2841, 1447, 1342, 1254, 1243, 976, 910, 890, 868, 826, 740; m/z (EI) 292 ([³⁰Si]M and [²⁹Si]M + H]⁺, 7%), 291 ([²⁹Si]M and M + H]⁺, 27), 290 (M⁺, 100), 217 (18), 165 (39), 149 (16), 135 (11), 83 (10), 73 (80); found M⁺ 290.2425, C₁₉H₃₄Si requires 290.2430. Anal. Calcd for C₁₉H₃₄Si: C, 78.54; H, 11.79. Found: C, 78.47; H, 11.57.

4-Methoxy-1-(trimethylsilyl)adamantane (9a): Photolysis of 3H-diazirine **1a** in MeOH afforded a mixture of *syn*- and *anti*-4-methoxy-1-(trimethylsilyl)adamantane (oil) *syn*-**9a**/*anti*-**9a** in 93% yield (ratio = 31:69). In addition, 3% of the intramolecular insertion products *s*-**7a** and *as*-**7a** were formed. These were separated by preparative GC on a 15% SE-30 column ($T_{\text{oven}} = 180$ °C, $T_{\text{injector}} = 220$ °C). Samples with purities of 100% (*anti*-**9a**) and 96% (*syn*-**9a**) were obtained.

anti-4-Methoxy-1-(trimethylsilyl)adamantane (anti-9a): $\delta_{\text{H}}/\text{ppm}$ (250.1 MHz, CDCl_3) –0.08 (9 H, s), 1.38–1.6 (6 H, m), 1.68–1.77 (3 H, m), 1.94–2.08 (4 H, m), 3.3 (1 H, s), 3.35 (3 H, s); $\delta_{\text{C}}/\text{ppm}$ (62.9 MHz, CDCl_3) –5.4 (–Si(CH₃)₃), 20.3 (C-1), 26.9 (C-7), 30.8 (C-3/C-5), 31.4 (C-6/C-10), 36.4 (C-2/C-9), 37.0 (C-8), 55.2 (–OCH₃), 83.4 (C-4); $\bar{\nu}_{\text{max}}/\text{cm}^{-1}$ (CCl₄) 2896, 2844, 1447, 1383,

1255, 1196, 1152, 1099, 1085, 1073, 934, 914, 866, 837; m/z (EI) 239 ($M+1$, 19), 238 (M^+ , 100), 223 (17), 206 (16), 165 (12), 134 (11), 133 (20), 110 (20), 92 (13), 91 (15), 89 (35), 79 (23), 78 (10), 73 (92); found M^+ 238.1749, $C_{14}H_{26}OSi$ requires 238.1753. Anal. Calcd for $C_{14}H_{26}OSi$: C, 70.52; H, 10.99. Found: C, 70.53; H, 10.84.

***syn*-4-Methoxy-1-(trimethylsilyl)adamantane (*syn*-9a):** δ_H /ppm (250.1 MHz, $CDCl_3$) -0.13 (9 H, s), 1.31 (2 H, d J 12.5), 1.56 (1 H, s), 1.62–1.70 (2 H, d J 11), 1.72–1.93 (5 H, m), 1.98 (2 H, s), 3.32 (4 H, s); δ_C /ppm (62.9 MHz, $CDCl_3$) -5.5 (–Si(CH₃)₃), 20.2 (C-1), 26.9 (C-7), 30.8 (C-3/C-5), 30.8 (C-2/C-9), 36.4 (C-6/C-10), 37.0 (C-8), 55.3 (–OCH₃), 83.2 (C-4); $\bar{\nu}_{max}/cm^{-1}$ (CCl_4) 2905, 2849, 2822, 1463, 1447, 1382, 1248, 1190, 1106, 1073, 902, 867, 841; m/z (EI) 239 ($M+1$, 17), 238 (M^+ , 81), 223 (84), 206 (16), 165 (16), 134 (16), 133 (16), 110 (15), 92 (20), 91 (23), 89 (37), 79 (34), 78 (16), 73 (100); found M^+ 238.1747, $C_{14}H_{26}OSi$ requires 238.1753.

5-(Trimethylsilyl)adamantan-2-one azine (3a):³² mp 188–190 °C; δ_H /ppm (400.13 MHz, $CDCl_3$) -0.13 (9 H, s), 1.64–1.94 (11 H, m), 2.58 (1 H, s), 3.23 (1 H, s); δ_C /ppm (100.6 MHz, $CDCl_3$) -5.4 (–Si(CH₃)₃), 21.4 (C-5), 31.4, 39.2 (C-1/C-3), 36.2 (C-6), 37.7, 37.9 (C-4/C-4'), 38.2, 38.3 (C-10/C-10'), 39.04, 39.07 (C-9/C-9'), 27.3 (C-7), 39.62, 39.64 (C-8/C-8'), 171.4, 171.6 (C-2/C-2'); $\bar{\nu}_{max}/cm^{-1}$ (KBr) 2922, 2840, 1645, 1455, 1342, 1250, 1077, 995, 961, 865, 832, 738, 626; m/z (EI) 440 (M^+ , 12%), 275 (10), 268 (14), 238 (10), 237 (40), 236 (32), 147 (12), 145 (12), 131 (12), 86 (22), 84 (34), 73 (100); found M^+ 440.3055, $C_{26}H_{44}N_2Si_2$ requires 440.3043.

Preparation and Reactions of 4-Azi-1-methyladamantane (1c): 3*H*-Diazirine 1c was synthesized from ketone 4c (52% yield)⁷² and purified by chromatography (silica gel 60, 230–400 mesh) using pentane as eluant to give a transparent, low-melting solid: mp 41–42 °C; δ_H /ppm (400.13 MHz, $CDCl_3$) 0.64 (2 H, s), 0.86 (3 H, s), 1.44 (2 H, dm J 13), 1.52 (2 H, s), 1.62 (2 H, dm J 12.5), 1.79 (2 H, d J 11.6), 1.99 (2 H, d J 11.6), 2.07–2.11 (1 H, m); δ_C /ppm (100.6 MHz, $CDCl_3$) 28.2 (C-7), 30.0 (C-1), 30.5 (–CH₃), 34.5 (C-6/C-10), 34.8 (C-3/C-5), 35.3 (C-4), 41.9 (C-2/C-9), 43.9 (C-8); $\bar{\nu}_{max}/cm^{-1}$ (KBr) 2920, 2849, 1574, 1538, 1455, 1376, 1358, 1098, 984, 934, 879, 842, 626; λ_{max}/nm (c- C_6H_{12}) 353 ($\epsilon/(10^4 M^{-1}cm^{-1})$ 0.16), 359 ($\epsilon/(10^4 M^{-1}cm^{-1})$ 0.13), 372 ($\epsilon/(10^4 M^{-1}cm^{-1})$ 0.22); m/z (EI) 148 ($[M - N_2]^+$, 19), 133 (27), 107 (29), 106 (42), 105 (48), 94 (19), 93 (69), 92 (89), 91 (100), 81 (12), 80 (28), 79 (60); found $[M - N_2]^+$ 148.1249, $C_{11}H_{16}$ requires 148.1252. Anal. Calcd for $C_{11}H_{16}N_2$: C, 74.96; H, 9.15; N, 15.89. Found: C, 75.06; H, 9.07; N, 16.04.

Gas-phase pyrolysis of 3*H*-diazirine 1c afforded *s*-7c and *as*-7c in a yield of 52%. Separation of the products *s*-7c and *as*-7c (2:1, respectively by NMR) was not possible. Even analytical GC was not able to separate the peaks at 50 °C, where they only started to get slightly asymmetrical. The mixture of the insertion products, therefore, had to be analyzed by 2-D NMR and proved to be identical with published results.²⁰ The IR shows the characteristic bands for the three-membered rings at 3027 cm^{-1} .

2,4-Didehydro-7-methyladamantane (*s*-7c): δ_H /ppm (600.1, $CDCl_3$) 0.73 (3 H, s), 1.05 (2 H, s), 1.12 (2 H, d J 12.5), 1.31–1.33 (2 H, m), 1.39 (2 H, s), 1.49 (2 H, s), 2.04 (1 H, s), 2.29 (2 H, s); δ_C /ppm (150.9 MHz, $CDCl_3$) 23.8 (C-2/C-4), 24.0 (C-3), 30.0 (C-7), 31.4 (–CH₃), 33.5 (C-1, C-5), 36.5 (C-10), 41.0 (C-6/C-8), 52.5 (C-9).

2,4-Didehydro-1-methyladamantane (*as*-7c): δ_H /ppm (600.1, $CDCl_3$) 1.07–1.08 (4 H, m), 1.12 (1 H, s), 1.23 (1 H, d J 9.8), 1.26–1.38 (4 H, m), 1.49 (1 H, s), 1.79 (2 H, s), 1.90 (1 H, s), 2.02 (1 H, s), 2.22 (1 H, s); δ_C /ppm (150.9 MHz, $CDCl_3$) 20.5 (C-3), 24.9 (C-4), 27.2 (C-7), 27.3 (–CH₃), 28.8 (C-10), 29.1 (C-2), 32.5 (C-6), 32.6 (C-5), 37.1 (C-1), 41.0 (C-8), 59.0 (C-9); $\bar{\nu}_{max}/cm^{-1}$ (CCl_4) 3027, 2995, 2924, 2847, 1454, 1372, 1358, 1336, 1034, 907; m/z (EI) 149 ($M+1$, 7), 148 (M^+ , 69), 133 (32), 119 (15), 107 (34), 106 (48), 105 (40), 94 (31), 93 (61), 92 (63), 91 (71), 80 (18), 79 (100), 77 (35); found M^+ 148.1255, $C_{11}H_{16}$ requires 148.1252.

***syn*-4-Cyclohexyl-1-methyladamantane (*syn*-8c):** The crude product mixture was chromatographed (silica gel 60, 230–400 mesh) using hexane as eluant and gave *syn*-8c/*anti*-8c (ratio = 3:2, respectively) in 65% (35% isolated yield). In addition, azines 3c (19–29%) and ketone 4c (10–19%) were formed. Analyses were done upon the

mixture: *syn*-4-cyclohexyl-1-methyladamantane (*syn*-8c) (major) and *anti*-4-cyclohexyl-1-methyladamantane (*anti*-8c) (minor). The diastereomers were differentiated using 2-D NMR techniques: δ_H /ppm (600.1 MHz, $CDCl_3$) 0.73–0.74 (5 H, m), 1.07–1.18 (4 H, m), 1.20 (2 H, d J 13), 1.37–1.38 (3 H, m), 1.49 (2 H, d J 12), 1.58 (2 H, d J 11.5), 1.61–1.75 (5 H, m), 1.77–1.83 (2 H, m), 1.88–1.90 (1 H, m), 1.95 (2 H, s); δ_C /ppm (150.9 MHz, $CDCl_3$) 26.6 (C-3'/C-5'), 26.8 (C-4'), 28.8 (C-7), 29.2 (C-3/C-5), 29.4 (C-1), 30.8 (C-2'/C-6'), 31.5 (–CH₃), 36.5 (C-1'), 38.6 (C-6/C-10), 39.0 (C-2/C-9), 45.4 (C-8), 48.8 (C-4); $\bar{\nu}_{max}/cm^{-1}$ (CCl_4) 2920, 2849, 1552, 1455, 1358, 1260, 1219, 1110, 1030, 982; m/z (EI) 232 (M^+ , 14), 217 (25), 150 (15), 149 (100), 93 (17), 82 (21); found M^+ 232.2188, $C_{17}H_{28}$ requires 232.2191.

***anti*-4-Cyclohexyl-1-methyladamantane (*anti*-8c):** δ_H /ppm (600.1 MHz, $CDCl_3$) 0.75–0.77 (5 H, m), 1.08–1.09 (1 H, m), 1.18–1.22 (3 H, m), 1.31 (2 H, d J 12.6), 1.38–1.42 (4 H, m), 1.44–1.46 (1 H, m), 1.52 (2 H, s), 1.62–1.64 (1 H, m), 1.70–1.74 (4 H, m), 1.81–1.85 (3 H, m), 1.93 (2 H, s); δ_C /ppm (150.9 MHz, $CDCl_3$) 26.7 (C-3'/C-5'), 26.8 (C-4'), 28.5 (C-7), 29.1 (C-3/C-5), 29.7 (C-1), 31.0 (CH₃, C-2'/C-6'), 31.3 (C-6/C-10), 36.4 (C-1'), 45.3 (C-8), 46.3 (C-2/C-9), 49.1 (C-4); m/z (EI) 232 (M^+ , 15), 217 (27), 150 (13), 149 (100), 93 (17), 82 (23).

The products from the insertion reaction of 5-methyladamantan-2-ylidene into MeOH (*syn*-9c/*anti*-9c) were isolated in a total yield of 84%. In addition, (according to GC analysis) 5% of the pyrolytic insertion products *syn*-9c and *anti*-9c were formed. After chromatography with pentane/ CH_2Cl_2 (9:1) on silica gel 60 (230–400 mesh) the mixture was analyzed: *syn*-4-methoxy-1-methyladamantane (*syn*-9c) and *anti*-4-methoxy-1-methyladamantane (*anti*-9c) were formed in a ratio of 3:2.

***syn*-4-Methoxy-1-methyladamantane (*syn*-9c):** δ_H /ppm (600.1, $CDCl_3$) 0.72 (3 H, s), 1.18 (2 H, d J 12.4), 1.39 (2 H, s), 1.58 (2 H, d J 12), 1.69–1.72 (4 H, m), 1.85 (1 H, s), 2.06 (2 H, s), 3.22 (1 H, s), 3.30 (3 H, s); δ_C /ppm (150.9 MHz, $CDCl_3$) 28.4 (C-7), 29.5 (C-1), 31.4 (–CH₃), 32.3 (C-3/C-5), 36.1 (C-6/C-10), 38.7 (C-2/C-9), 44.9 (C-8), 55.7 (–OCH₃), 82.8 (C-4); m/z (EI) 180 (M^+ , 15), 165 (5), 149 (18), 148 (100), 133 (23), 107 (13), 106 (24), 105 (20), 93 (31), 92 (26), 91 (20), 79 (18). From the mixture: found M^+ 180.1517, $C_{12}H_{20}O$ requires 180.1514.

***anti*-4-Methoxy-1-methyladamantane (*anti*-9c):** δ_H /ppm (600.1, $CDCl_3$) 0.77 (3 H, s), 1.32 (2 H, d J 12), 1.36–1.38 (2 H, m), 1.44 (2 H, s), 1.49 (2 H, d J 13.4), 1.83 (1 H, s), 1.94 (2 H, J 11.3), 2.01 (2 H, s), 3.26 (1 H, s), 3.31 (3 H, s); δ_C /ppm (150.9 MHz, $CDCl_3$) 28.4 (C-7), 29.6 (C-1), 30.8 (–CH₃), 31.1 (C-6/C-10), 32.0 (C-3/C-5), 43.6 (C-2/C-9), 44.9 (C-8), 55.8 (–OCH₃), 83.4 (C-4); $\bar{\nu}_{max}/cm^{-1}$ (CCl_4) from the mixture (*anti*-9c/*syn*-9c) 2915, 2849, 1454, 1381, 1197, 1104, 1086; m/z (EI) 180 (M^+ , 14), 165 (6), 149 (18), 148 (100), 133 (23), 107 (11), 106 (24), 105 (21), 93 (30), 92 (25), 91 (20).

5-Methyladamantan-2-one azine (3c): δ_H /ppm (400.13 MHz, $CDCl_3$) 0.76–0.81 (3 H, s), 1.50–2.10 (11 H, m), 2.59 (1 H, s), 3.24 (1 H, s); δ_C /ppm (100.6 MHz, $CDCl_3$) 39.6, 31.6 (C-1/C-3); 43.3 (C-6); 44.50, 44.53, 45.7 (C-4/C-9); 38.6, 37.3 (C-8/C-10), 28.5 (C-7), 30.0 (C-5); 170.9, 170.8 (C-2, C-2'); IR (KBr) 2908, 2844, 1647, 1453, 1375, 1356, 1182, 1104, 1084, 939 cm^{-1} ; (EI) m/z 325 ($M+1$, 17), 324 (M^+ , 76), 323 (15), 281 (22), 267 (43), 253 (15), 229 (15), 240 (25), 190 (15), 189 (54), 164 (100), 163 (28), 162 (35); found M^+ 324.2572, $C_{22}H_{32}N_2$ requires 324.2565.

Preparation and Reactions of 4-Azadamantan-1-amine (1d):^{24a} 3*H*-Diazirine 1d was synthesized in 26% yield from ketone 4d. The crude product, which contained 7% of 4-azadamantan-1-ol byproduct, was chromatographed (silica gel 60, 230–400 mesh) using a mixture of methanolic NH_3 (0.7 M) and EtOAc (7:11) as eluant and a solid, which sublimed at reduced pressure, was obtained: mp 130 °C dec; δ_H /ppm (250.1 MHz, $CDCl_3$) 0.76 (2 H, s), 1.61 (2 H, d J 13.6), 1.67 (2 H, d J 14.8), 1.70 (2 H, s), 1.96 (2 H, d J 12.3), 2.01 (2 H, d J 11.3), 2.25 (1 H, s), (NH_2 -group not obsd); δ_C /ppm (62.9 MHz, $CDCl_3$) 29.1 (C-7), 34.0 (C-6/C-10), 35.5 (C-3/C-5), 43.6 (C-2/C-9), 45.4 (C-8), 47.4 (C-1), (C-4 not obsd); $\bar{\nu}_{max}/cm^{-1}$ (KBr) 3355, 3265, 2922, 2854, 1575, 1449, 1350, 1293, 1132, 1108, 1067, 926;

$\lambda_{\text{max}}/\text{nm}$ (*c*-C₆H₁₂) 352 ($\epsilon/(10^4 \text{ M}^{-1}\text{cm}^{-1})$ 0.26), 356 ($\epsilon/(10^4 \text{ M}^{-1}\text{cm}^{-1})$ 0.24), 370 ($\epsilon/(10^4 \text{ M}^{-1}\text{cm}^{-1})$ 0.31); m/z (CI) 178 ($[\text{M} + \text{H}]^+$, 100), 165 (64), 149 (92). Anal. Calcd for C₁₀H₁₅N₃: C, 67.76; H, 8.53; N, 23.71. Found: C, 67.61; H, 8.50; N, 23.45.

2,4-Didehydroadamantan-7-amine (s-7d): Pyrolysis of 3*H*-diazirine **1d** gave 1,3-CH insertion products *s*-7d and *as*-7d in 89% yield (ratio = 4:1). By using preparative GC (Carbowax/KOH, $T_{\text{oven}} = 140^\circ\text{C}$, $T_{\text{injector}} = 260^\circ\text{C}$) a sample of the major product was obtained (the minor product was enriched, vide infra): $\delta_{\text{H}}/\text{ppm}$ (600.13 MHz, CDCl₃) 1.16 (2 H, d J 12.1), 1.27–1.31 (2 H, m), 1.34 (1 H, dm J 10), 1.40 (2 H, m), 1.5 (1 H, m), 1.61–1.64 (2 H, m), 2.02–2.07 (1 H, m), 2.41 (2 H, s), (NH₂-group not obsd); $\delta_{\text{C}}/\text{ppm}$ (150.9 MHz, CDCl₃) 23.0 (C-2/C-4), 25.6 (C-3), 34.4 (C-1/C-5), 37.5 (C-10), 42.6 (C-6/C-8), 48.2 (C-7), 51.5 (C-9); $\bar{\nu}_{\text{max}}/\text{cm}^{-1}$ of mixture (CDCl₃) 3356, 3032, 2934, 2850, 1442, 1356, 1334, 1141; m/z (EI) 150 ($[\text{M} + \text{H}]^+$, 11), 149 (M^+ , 100), 148 (37), 134 (19), 117 (16), 108 (16), 107 (66), 106 (97), 94 (56), 93 (13), 91 (17), 77 (13), 61 (14); found M^+ 149.1199, C₁₀H₁₅N requires 149.1204.

2,4-Didehydroadamantan-1-amine (as-7d): $\delta_{\text{H}}/\text{ppm}$ (600.13 MHz, CDCl₃) 1.18–1.30 (3 H, m), 1.31–1.35 (2 H, m), 1.46 (1 H, d J 12), 1.53–1.59 (2 H, m), 1.76–1.85 (2 H, m), 2.02 (1 H, s), 2.21–2.23 (2 H, m), (NH₂-group not obsd); $\delta_{\text{C}}/\text{ppm}$ (150.9 MHz, CDCl₃) 20.2 (C-3), 24.3 (C-4), 27.4 (C-7), 28.4 (C-10), 30.2 (C-2), 31.6 (C-5), 31.9 (C-6), 42.0 (C-8), 55.2 (C-1), 59.5 (C-9); m/z (EI) 149 (M^+ , 6.6), 94 (12), 93 (13), 61 (100), 60 (10); found M^+ 149.1209, C₁₀H₁₅N requires 149.1204.

syn-4-Cyclohexyladamantan-1-amine (syn-8d): Product mixture *syn*-8d/*anti*-8d (ratio = 89:11, respectively) was isolated in 48% yield. In addition, 32% of ketone **4d**^{24a} was formed. Separation using preparative GC (Carbowax/KOH) failed. Only the major product could be enriched (>90%): $\delta_{\text{H}}/\text{ppm}$ (600.13 MHz, CDCl₃) 0.60–0.75 (2 H, m), 1.05–1.18 (4 H, m), 1.29 (2 H, d J 11.7) 1.33–1.39 (1 H, m), 1.48–1.58 (4 H, m), 1.58–1.65 (5 H, m), 1.66 (2 H, m), 1.78 (2 H, d J 11.7), 2.01 (1 H, s), 2.07 (2 H, s), (NH₂-group not obsd); $\delta_{\text{C}}/\text{ppm}$ (150.9 MHz, CDCl₃) 26.6 (C-3'/C-5'), 26.7 (C-4'), 29.8 (C-7), 30.3 (C-3/C-5), 30.7 (C-2'/C-6'), 36.5 (C-1'), 37.9 (C-6/C-10), 40.6 (C-2/C-9) 47.0 (C-8), 48.4 (C-4), (C-1 not obsd); $\bar{\nu}_{\text{max}}/\text{cm}^{-1}$ (CDCl₃) 3355, 2921, 2851, 1449, 1359, 1304, 1182, 1115, 1098, 1048, 990, 952, 932, 912, 734, 530; m/z (EI) 234 ($[\text{M} + \text{H}]^+$, 7), 233 (M^+ , 43), 176 (15), 95 (10), 94 (100), 61 (22); found M^+ 233.2149, C₁₆H₂₇N requires 233.2143.

anti-4-Cyclohexyladamantan-1-amine (anti-8d): $\delta_{\text{H}}/\text{ppm}$ (600.13 MHz, CDCl₃) 0.64–0.78 (2 H, m), 1.02–1.18 (4 H, m), 1.23–1.27 (2 H, m), 1.35–1.41 (1 H, m), 1.43–1.57 (4 H, m), 1.58–1.68 (5 H, m), 1.69–1.73 (2 H, m), 1.77–1.79 (2 H, m), 1.96 (1 H, s), 2.03 (2 H, s), (NH₂-group not obsd); $\delta_{\text{C}}/\text{ppm}$ (150.9 MHz, CDCl₃) 26.6 (C-3'/C-5'), 26.7 (C-4'), 29.3 (C-7), 30.0 (C-3/C-5), 30.6 (C-2'/C-6'), 30.9 (C-6/C-10), 36.3 (C-1'), 47.2 (C-8), 47.5 (C-2/C-9), 48.4 (C-4); (C-1 not obsd); m/z (EI) 233 (M^+ , 30), 176 (20), 94 (100); found M^+ 233.2151, C₁₆H₂₇N requires 233.2143.

syn-4-Methoxyadamantan-1-amine (syn-9d): Photolysis of 3*H*-diazirine **1d** in MeOH afforded *syn*-9d and *anti*-9d in a combined yield of 93% (ratio = 3:1). Separation using preparative GC (Carbowax/KOH) failed. However, enriched fractions of the major (98%) and minor (70%) products were analyzed: $\delta_{\text{H}}/\text{ppm}$ (400.13 MHz, CDCl₃) 1.15 (2 H, s), 1.24 (2 H, d J 12), 1.45–1.53 (4 H, m), 1.62 (2 H, d J 11.8), 1.77 (2 H, d J 11.1), 1.91 (1 H, s), 2.12 (2 H, s), 3.10–3.14 (1 H, m), 3.24 (3 H, s); $\delta_{\text{C}}/\text{ppm}$ (100.6 MHz, CDCl₃) 28.9 (C-7), 33.0 (C-3/C-5), 35.1 (C-6/C-10), 40.4 (C-2/C-9), 45.6 (C-8), 55.2 (–OCH₃), 81.5 (C-4), (C-1 not obsd); $\bar{\nu}_{\text{max}}/\text{cm}^{-1}$ of mixture (CCl₄) 3367, 2912, 2853, 1615, 1450, 1360, 1106; m/z (EI) 182 ($[\text{M} + \text{H}]^+$, 8), 181 (M^+ , 61), 124 (24), 95 (10), 94 (100); found M^+ 181.1472, C₁₁H₁₉NO requires 181.1467.

anti-4-Methoxyadamantan-1-amine (anti-9d): $\delta_{\text{H}}/\text{ppm}$ (400.13 MHz, CDCl₃) 1.20–1.27 (4 H, m), 1.50–1.55 (6 H, m), 1.85–1.92 (3 H, m), 2.05 (2 H, s), 3.21–3.27 (4 H, m); $\delta_{\text{C}}/\text{ppm}$ (100.61 MHz, CDCl₃) 29.0 (C-7), 30.2 (C-6/C-10), 32.4 (C-3/C-5), 44.7 (C-2/C-9), 46.5 (C-8), 56.5 (–OCH₃), 82.4 (C-4), (C-1 not obsd); m/z (EI) 182 ($[\text{M} + \text{H}]^+$, 6), 181 (M^+ , 54), 124 (48), 109 (10), 95 (11), 94 (100); found M^+ 181.1471, C₁₁H₁₉NO requires 181.1467.

5-Aminoadamantan-2-one azine (3d): mp 249–253 °C; $\delta_{\text{H}}/\text{ppm}$ (400.13 MHz, CDCl₃) 1.50–1.90 (10 H, m), 2.20 (1 H, s), 2.59 (1 H, s), 3.24 (1 H, s), (NH₂-group not obsd); $\delta_{\text{C}}/\text{ppm}$ (100.6 MHz, CDCl₃) 29.5 (C-7), 32.1 (C-3), 36.93, 36.96 (C-10/C-10'), 38.2 (C-8), 40.1 (C-1), 45.24, 45.27 (C-6/C-6'), 45.8, 45.87 (C-4/C-4'), 46.93, 46.94 (C-9/C-9'), 47.4 (C-NH₂), 170.1 (C-2); $\bar{\nu}_{\text{max}}/\text{cm}^{-1}$ (KBr) 3442, 2924, 2850, 1644, 1445, 1357, 1141, 1089, 1074, 955; m/z (EI) 327 ($[\text{M} + \text{H}]^+$, 15.5), 326 (M^+ , 100), 205 (10), 165 (11), 163 (52), 94 (22); found M^+ 326.2463, C₂₀H₃₀N₄ requires 326.2470.

Preparation and Reactions of 4-Aziadamantan-1-ol (1e):^{21a} 3*H*-Diazirine **1e** was synthesized in 46% yield from ketone **4e**.⁷³ Purification by chromatography with Et₂O/ligroin (8:2) on silica gel 60 (230–400 mesh) gave a readily crystallizing white solid (mp 140 °C dec). The pyrolytic reactions of **1e** afforded intramolecular insertion products *s*-7e and *as*-7e in 94% yield (ratio = 9:1). Analyses were done on the mixture. The products *syn*-8e and *anti*-8e (ratio = 89:11) from the insertion reaction of 5-hydroxyadamantan-2-ylidene into cyclohexane were isolated in a total yield of 92%. In addition, traces of azines **3e** were formed and 6% of ketone **4e**. After chromatography on silica gel 60 (230–400 mesh) with ligroin/EtOAc (85:15), *syn*-cyclohexyladamantan-1-ol (*syn*-8e) was isolated in 21% yield. Photolysis of **1e** in MeOH afforded *syn*-9e and *anti*-9e in 97% yield (ratio = 3:1). After chromatography on silica gel 60 (230–400 mesh) using ligroin/EtOAc (8:2), *syn*-9e was isolated in 21% yield and *anti*-9e in 7% yield.

5-Hydroxyadamantan-2-one azine (3e): mp 250 °C (sublimes), 305 °C dec; $\delta_{\text{H}}/\text{ppm}$ (250.13 MHz, CDCl₃) 3.47 (1 H, “s”), 2.82 (1 H, “s”), 2.30 (1 H, “s”), 1.60–1.95 (11 H, m); $\delta_{\text{C}}/\text{ppm}$ (62.9 MHz, CDCl₃) 30.7, 33.0, 37.2, 38.5, 41.0, 44.7, 45.0, 46.1, 68.2, 170.1; $\bar{\nu}_{\text{max}}/\text{cm}^{-1}$ (KBr) 3386, 2923, 2853, 1646, 1451, 1352, 1291, 1115, 1093, 1067, 971, 926; m/z (EI) 329 ($[\text{M} + \text{H}]^+$, 21), 328 (M^+ , 88), 282 (11), 279 (14), 167 (24), 166 (55), 165 (11), 164 (27), 151 (13), 150 (17), 149 (59), 148 (12), 109 (17), 108 (21), 107 (17), 97 (25), 96 (24), 95 (100), 94 (26), 83 (20), 71 (29), 70 (20), 69 (30), 67 (25), 57 (45), 55 (40); found M^+ 328.2157, C₂₀H₂₈N₂O₂ requires 328.2151.

Reactions of 4-Azi-1-bromoadamantane (1f) and 4-Azi-1-chloroadamantane (1g): The preparation and reaction of 3*H*-diazirines **1f** and **1g** were performed in the usual manner (vide supra).^{24b,68} Their respective reaction products were studied using GC and GC–MS. The insertion products with MeOH are described elsewhere.^{17a}

Intramolecular Insertion Reaction Products: The intramolecular insertion products are formed in the injector unit of the analytic GC and GC–MS, respectively: *s*-7f m/z (EI) 214, 212 (M^+ , 6), 134 (10), 133 (91), 117 (11), 105 (18), 91 (65), 79 (100), 78 (62); *as*-7f m/z (EI) 214, 212 (M^+ , 12, 10), 172, 170 (12), 157 (14), 133 (100), 117 (28), 115 (12), 105 (19), 103 (12), 92 (18), 91 (60), 79 (33), 77 (19); *s*-7g m/z (EI), 168 (M^+ , 16), 133 (11), 127 (10), 126 (20), 117 (15), 105 (14), 92 (25), 91 (76), 79 (100), 78 (74), 77 (25).

Insertion into Cyclohexane: *syn*-8g m/z (EI) 252 (M^+ , 5) 218 (18), 217 (100), 169 (22), 135 (20), 134 (22), 133 (23), 93 (14), 92 (14), 91 (34), 83 (25), 82 (37), 79 (31); *anti*-8g m/z (EI) 252 (M^+ , 9) 218 (19), 217 (100), 169 (20), 135 (19), 133 (27), 115 (10), 105 (11), 93 (14), 92 (10), 91 (33), 83 (22), 82 (32), 79 (31); *syn*-8f m/z (EI) 218 (M^+ -Br, 20), 217 (100), 161 (7), 149 (8), 135 (29), 121 (16), 93 (15), 91 (14), 81 (10), 79 (20); *anti*-8f m/z (EI) 218 (M^+ -Br, 14), 217 (100), 161 (7), 135 (32), 121 (13), 93 (11), 91 (14), 81 (13), 79 (17).

Insertion into Methanol: *syn*-9f m/z (EI) 166 ($\text{M} + 1 - \text{Br}$, 11), 165 ($\text{M}^+ - \text{Br}$, 100), 133 (12), 109 (9), 105 (10), 91 (11); *anti*-9f m/z (EI) 166 ($\text{M} + 1 - \text{Br}$, 12), 165 ($\text{M}^+ - \text{Br}$, 100), 133 (45), 105 (12), 91 (27), 79 (13); *rearr*-9f m/z (EI) 214, 212 (M^+ , OCH₃, 20), 165 (38), 133 (100), 109 (13), 105 (14), 91 (38), 79 (44), 78 (26); *syn*-9g m/z (EI) 200 (M^+ , 13), 170 (31), 168 (100), 165 (23), 133 (40), 126 (17), 105 (11), 92 (16), 91 (43), 79 (28), 78 (17); *anti*-9g m/z (EI) 200 (M^+ , 21), 170 (36), 168 (100), 165 (21), 133 (42), 126 (21), 105 (11), 92 (17), 91 (48), 79 (24), 78 (17).

The preparation of 4-azi-1-fluoroadamantane (**1h**) has been discussed thoroughly in the Supporting Information of a recent publication.^{24b} Only the products from (**1h**) are described here.

Preparation and Reactions of 4-Azi-1-fluoroadamantane (1h): ^{48e} 3H-Diazirine **1h** was synthesized from ketone **4h**. The crude product was chromatographed (silica gel 60, 230–400 mesh) using pentane as eluant and a readily crystallizing white solid (mp 60 °C (sublimes)) was obtained in 44% yield. The pyrolytic intramolecular insertion reactions of **1h** afforded *s*-**7h** and *as*-**7h** in 43% in yield (ratio =92:8); separation of these products was not possible. The *s*-**7h**/*as*-**7h** mixture was analyzed using 2-D NMR.

2,4-Didehydro-7-fluoroadamantane (s-7h): δ_{H} /ppm (600.13 MHz, CDCl₃) 1.43 (3 H, m), 1.50 (2 H, d J 10.3), 1.61–1.66 (3 H, m), 1.97–1.99 (2 H, m), 2.07 (1 H, s), 2.59 (2 H, s); δ_{C} /ppm (150.9 MHz, CDCl₃) 23.4 (*J*_{CF} 1.6; C-2/C-4), 28.5 (*J*_{CF} 11.3; C-3), 34.8 (*J*_{CF} 19.8; C-10), 36.6 (*J*_{CF} 9.3; C-1/C-5), 39.1 (*J*_{CF} 17.6; C-6/C-8), 51.2 (*J*_{CF} 2.2; C-9), 91.4 (*J*_{CF} 180.3; C-7); $\bar{\nu}_{\text{max}}$ /cm⁻¹ (CCl₄) 3034, 2942, 2864, 1458, 1448, 1352, 1333, 1247, 1086, 1054, 975, 926, 891; *m/z* (EI) 152 (*M*⁺, 78), 137 (14), 117 (10), 111 (35), 110 (55), 109 (49), 98 (27), 97 (100), 93 (15), 92 (53), 91 (60), 80 (11), 79 (26), 77 (28), found *M*⁺ 152.0998, C₁₀H₁₃F requires 152.1001.

2,4-Didehydro-1-fluoroadamantane (as-7h): Obtained from a concentrated solution containing 8% of *as*-**7h**: δ_{H} /ppm (600.1 MHz, CDCl₃) 1.22 (1 H, s), 1.25 (1 H, s), 1.32 (1 H, s), 1.57–1.58 (2 H, m), 1.6 (1 H, br s), 1.75–1.80 (3 H, m), 1.86 (1 H, m), 2.14 (1 H, s), 2.30 (1 H, s), 2.57 (1 H, s); δ_{C} /ppm (150.9 MHz, CDCl₃) 19.7 (C-3), 22.3 (*J*_{CF} 1.2; C-4), 26.4 (*J*_{CF} 31; C-2), 28.0 (*J*_{CF} 1.4; C-7), 28.6 (*J*_{CF} 11; C-10), 30.3 (*J*_{CF} 9.1; C-5), 33.7 (*J*_{CF} 2.7; C-6), 36.5 (*J*_{CF} 18.7; C-8), 55.6 (*J*_{CF} 17.7; C-9), 92.3 (*J*_{CF} 180; C-1); *m/z* (EI) 152 (*M*⁺, 89), 137 (18), 117 (12), 111 (17), 110 (86), 109 (73), 98 (23), 97 (100), 93 (27), 92 (83), 91 (68), 80 (15), 79 (72), 78 (15), 77 (36).

syn-4-Cyclohexyl-1-fluoroadamantane (syn-8h): The insertion reaction of 5-fluoroadamantan-2-ylidene into cyclohexane produced a crude mixture that consisted of mostly *syn*-**8h**/*anti*-**8h** (76%, ratio =92:8) with lesser amounts of azines **3h** (11%), ketone **4h** (4%), and unreacted starting material (7%). It was chromatographed (silica gel 60, 230–400 mesh) using pentane as eluant and the readily crystallizing solid *syn*-**8h** (mp 54–56 °C) was isolated in 46% yield: δ_{H} /ppm (600.1 MHz, CDCl₃) 0.73 (2 H, m), 1.00–1.20 (4 H, m), 1.30–1.40 (1 H, m), 1.54 (2 H, d J 14.9), 1.55–1.72 (7 H, m), 1.80–1.83 (4 H, m), 1.98 (2 H, s), 2.19 (1 H, s), 2.26 (2 H, s); δ_{C} /ppm (150.9 MHz, CDCl₃) 26.5 (C-3'/C-5'), 26.6 (C-4'), 30.6 (C-2'/C-6'), 31.5 (*J*_{CF} 9.8; C-7), 32.1 (*J*_{CF} 9.1; C-3/C-5), 36.5 (C-1'), 37.4 (*J*_{CF} 15.4; C-2/C-9), 37.5 (*J*_{CF} 3.8; C-6/C-10), 43.4 (*J*_{CF} 16.9; C-8), 48.2 (*J*_{CF} 1.7 Hz; C-4), 97.8 (*J*_{CF} 183.4 Hz; C-1); $\bar{\nu}_{\text{max}}$ /cm⁻¹ (CCl₄) 2932, 2852, 1452, 1355, 1304, 1184, 1110, 1085, 1048, 1030, 946, 908; *m/z* (EI) 237 ([*M* + *H*]⁺, 17), 236 (*M*⁺, 100), 153 (57), 152 (11), 135 (19), 134 (30), 133 (18), 97 (98), 93 (12), 91 (24), 88 (21); found *M*⁺ 236.1946, C₁₆H₂₅F requires 236.1940. Anal. Calcd for C₁₆H₂₅F: C, 81.30; H, 10.66. Found: C, 81.17; H, 10.90.

anti-4-Cyclohexyl-1-fluoroadamantane (anti-8h): The *syn*-**8h**/*anti*-**8h** mixture could be enriched in epimer *anti*-**8h**, which was characterized: δ_{H} /ppm (600.13 MHz, CDCl₃) 0.73 (2 H, mc), 1.11–1.18 (4 H, m), 1.32 (2 H, d J 12.7), 1.39–1.41 (1 H, m), 1.62–1.72 (5 H, m), 1.78–1.84 (8 H, m), 2.14 (1 H, s), 2.20 (2 H, s); δ_{C} /ppm (150.9 MHz, CDCl₃) 26.5 (C-4'), 26.6 (C-3'/C-5'), 30.3 (*J*_{CF} 2.3; C-6/C-10), 30.9 (C-2'/C-6'), 31.2 (*J*_{CF} 9.2; C-7), 31.5 (*J*_{CF} 9.7; C-3/C-5), 36.4 (*J*_{CF} 1.9; C-1'), 43.2 (*J*_{CF} 16.9; C-8), 43.4 (*J*_{CF} 17.5; C-2/C-9), 48.4 (*J*_{CF} 1.6; C-4), 92.3 (*J*_{CF} 186; C-1); *m/z* (EI) 237 ([*M* + *H*]⁺, 16), 236 (*M*⁺, 91), 154 (12), 153 (100), 152 (16), 135 (32), 134 (48), 133 (28), 97 (18), 93 (18), 92 (16), 91 (43), 83 (45), 82 (85), 80 (23).

1-Fluoro-4-methoxyadamantane (9h): The insertion reaction of 5-fluoroadamantan-2-ylidene into MeOH produced a crude mixture that consisted of mostly *syn*-**9h**/*anti*-**9h** (85%, ratio = 84:16) with lesser amounts of intramolecular insertion products (5%) and a rearrangement product (2%) that was further investigated from an enriched mixture obtained after chromatography (vide infra). It was chromatographed (silica gel 60, 230–400 mesh) using pentane/CH₂Cl₂ (9:1) as eluant and *syn*-**9h** was isolated in 50% overall yield.

syn-1-Fluoro-4-methoxyadamantane (syn-9h): δ_{H} /ppm (600.1 MHz, CDCl₃) 1.52 (2 H, d J 13.8), 1.59 (2 H, s), 1.68 (2 H, d J 12), 1.82 (2 H, s), 2.13–2.14 (3 H, m), 2.33 (2 H, s), 3.14 (1 H, s), 3.30 (3 H, s); δ_{C} /ppm (150.9 MHz, CDCl₃) 30.6 (*J*_{CF} 9.5; C-7), 34.6 (*J*_{CF} 2.2;

C-6/C-10), 34.7 (*J*_{CF} 9.9; C-3/C-5), 36.7 (*J*_{CF} 18; C-2/C-9), 42.6 (*J*_{CF} 17.5; C-8), 55.3 (–OCH₃), 80.8 (*J*_{CF} 2.3 C-4), 91.7 (*J*_{CF} 184 C-1); $\bar{\nu}_{\text{max}}$ /cm⁻¹ (CCl₄) 2922, 2860, 1451, 1381, 1355, 1193, 1106, 1072, 992, 924, 909; *m/z* (EI) 184 (*M*⁺, 15), 153 (13), 152 (100), 137 (10), 123 (21), 111 (13), 110 (22), 109 (15), 97 (24); found *M*⁺ 184.1260, C₁₁H₁₇OF requires 184.1262. Anal. Calcd for C₁₆H₂: C, 71.71; H, 9.31. Found: C, 71.86; H, 9.60.

anti-1-Fluoro-4-methoxyadamantane (anti-9h): δ_{H} /ppm (600.1 MHz, CDCl₃) 1.33 (2 H, d J 12.7), 1.84–1.88 (6 H, m), 1.93 (2 H, m), 2.13 (1 H, s), 2.23 (2 H, s), 3.31 (3 H, s) 3.32 (1 H, s); δ_{C} /ppm (150.9 MHz, CDCl₃) 29.8 (*J*_{CF} 2; C-6/C-10), 30.6 (*J*_{CF} 9.7; C-7), 33.6 (*J*_{CF} 10.4; C-3/C-5), 40.8 (*J*_{CF} 18.4; C-2/C-9), 42.7 (*J*_{CF} 16.6; C-8), 55.8 (–OCH₃), 81.5 (*J*_{CF} = 1.6; C-4), 91.9 (*J*_{CF} 183.6; C-1); *m/z* (EI) 184 (*M*⁺, 20), 153 (15), 152 (100), 110 (27), 109 (16), 97 (25), 92 (20), 91 (17).

It was possible to determine the structure of the protic rearrangement product *rearr*-**9h** by 2-D NMR (see ref 29 in Supporting Information) because it was enriched to 12% by chromatography.

7-Fluorotricyclo[3.3.1.1^{2,7}]decan-3-yl methyl ether (rearr-9h) (Table 15): *m/z* (EI) 184 (26), 153 (14), 152 (100), 137 (10), 123 (19), 111 (14), 110 (20), 109 (22), 98 (11), 97 (22), 93 (13), 92 (17), 91 (18), 84 (13), 79 (22).

Table 15. Chemical Shifts of 7-Fluorotricyclo[3.3.1.1^{2,7}]decan-3-yl Methyl Ether (*rearr*-9h**) Extracted from 2-D NMR**

<i>rearr</i> - 9h	δ_{C} (ppm)	H ₁	H ₂	<i>J</i> _{CF} (Hz)
1	91.6			179.4
9/10*	43.8	2.03	1.735	19.5
	45.6	2.11	1.52	16.2
2	37.7	1.984	1.434	19.8
4	78.6	3.48		
5	33.9	1.92	1.84	
7	30.9	1.92	1.2	2
6	26.9	2.14		11.9
8	33.8	2.265		9.7
3	31.1	2.615		7.5
OCH ₃	55.3	3.27		

5-Fluoroadamantan-2-one azine^{24b,74} (3h): 3H-Diazirine **1h** (20 mg, 0.11 mmol) was photolyzed in a cooled, rotating flask (*T* = 5 °C, 2 h). For GC and GC–MS analyses, the crude product was dissolved in CHCl₃. For NMR analyses, the crude product was washed with hot ligroin and dried in vacuo: δ_{H} /ppm (400.1 MHz, CDCl₃) 1.68 (2 H, s), 1.70–1.85 (6 H, m), 1.91–1.97 (4 H, m), 1.98–2.05 (8 H, m), 2.36 (2 H, s), 2.83 (2 H, s), 3.53 (2 H, s); δ_{C} /ppm (100.6 MHz, CDCl₃) 32.9 (*J*_{CF} 9.6; C-3), 31.0 (*J*_{CF} 9.2; C-7), 36.7, 37.9 (C-8/C-10), 41.0 (*J*_{CF} 9.9; C-1), 41.7 (*J*_{CF} = 19.7; C-6), 41.9, 42.9 (*J*_{CF} 20; C-4/C-9); 91.1, 91.2 (*J*_{CF} 185.5; C-5), 169.4 (C-2); λ_{max} /nm (C₆H₁₄) 211 (ϵ /(10⁴ M⁻¹cm⁻¹) 25), 232 (ϵ /(10⁴ M⁻¹cm⁻¹) 7.7).

■ ASSOCIATED CONTENT

Supporting Information

NMR, IR, UV spectra, GC–MS data of new compounds, and computational data. This material is available free of charge via the Internet at <http://pubs.acs.org>.

■ AUTHOR INFORMATION

Corresponding Author

*Phone: +43-1-4277-52121. Fax: + 43-1-4277-52140. E-mail: udo.brinker@univie.ac.at.

■ ACKNOWLEDGMENTS

We thank Mag. P. Billing for discussions, Dozent Dr. J.-L. Mieusset for his valuable help and support, and Dr. G. Wagner

of the Institute of Organic Chemistry of the University of Vienna for the preparation of compounds **1f** and **1g**.

REFERENCES

- (1) Carbene Rearrangements 84. For part 83, see: Gupta, S.; Choudhury, R.; Krois, D.; Wagner, G.; Brinker, U. H.; Ramamurthy, V. *Org. Lett.* **2011**, 13, 6074.
- (2) See the special issue devoted entirely to this topic: Diastereoselection; le Noble, W. J.; Gung, B. W., Eds. *Chem. Rev.* **1999**, 99, 1067–1480 and references therein.
- (3) Johnson, C. R.; Tait, B. D.; Cieplak, A. S. *J. Am. Chem. Soc.* **1987**, 109, 5875.
- (4) (a) Filippi, A.; Trout, N. A.; Brunelle, P.; Adcock, W.; Sorensen, T. S.; Speranza, M. J. *Org. Chem.* **2004**, 69, 5537. (b) Adcock, W.; Trout, N. A. *J. Org. Chem.* **1991**, 56, 3229. (c) Laube, T.; Stilz, H. U. *J. Am. Chem. Soc.* **1987**, 109, 5876.
- (5) (a) Kaselj, M.; Chung, W.-S.; le Noble, W. J. *Chem. Rev.* **1999**, 99, 1387. (b) According to the IUPAC, steric effect refers to “the effect on a chemical or physical property (structure, rate or equilibrium constant) upon introduction of substituents having different steric requirements. Steric effects arise from contributions ascribed to strain as the sum of (1) non-bonded repulsions, (2) bond angle strain, and (3) bond stretches or compressions. A “secondary steric effect” involves the differential moderation of electron delocalization by non-bonded compressions.
- (6) Stereoelectronic effects arise from the different alignment of electronic orbitals in different arrangements of nuclear geometry. Moss, G. P. *Pure Appl. Chem.* **1996**, 68, 2193 (basic terminology of stereochemistry (IUPAC Recommendations 1996), p 2218).
- (7) Cieplak, A. S.; Tait, B. D.; Johnson, C. R. *J. Am. Chem. Soc.* **1989**, 111, 8447.
- (8) (a) Anh, N. T. *Top. Curr. Chem.* **1980**, 88, 145. (b) Anh, N. T.; Eisenstein, O. *Nouv. J. Chim.* **1977**, 1, 61. (c) Anh, N. T.; Eisenstein, O. *Tetrahedron Lett.* **1976**, 3, 155. (d) Cieplak, A. S. *J. Am. Chem. Soc.* **1981**, 103, 4540.
- (9) Anh, N. T. *Frontier Orbitals: A Practical Manual*; Wiley: Chichester, 2007.
- (10) Yadav, V. K.; Gupta, A.; Balamurugan, R.; Sriramurthy, V.; Kumar, N. V. *J. Org. Chem.* **2006**, 71, 4178.
- (11) Kaneno, D.; Tomoda, S. *Tetrahedron Lett.* **2004**, 45, 4559.
- (12) Kaneno, D.; Tomoda, S. *Org. Lett.* **2003**, 5, 2947.
- (13) (a) Tomoda, S. *Chem. Rev.* **1999**, 99, 1243. (b) Tomoda, S.; Senju, T. *Tetrahedron* **1999**, 55, 5303.
- (14) (a) Klopman, G.; Hudson, R. F. *Theor. Chim. Acta* **1967**, 8, 165. (b) Klopman, G. *J. Am. Chem. Soc.* **1968**, 90, 223. (c) Salem, L. *J. Am. Chem. Soc.* **1968**, 90, 543. (d) Fleming, I. *Frontier Orbitals and Organic Chemical Reactions*; Wiley: London, 1976.
- (15) (a) Suzuki, Y.; Kaneno, D.; Tomoda, S. *J. Phys. Chem. A* **2009**, 113, 2578. (b) Cheung, C. K.; Tseng, L. T.; Lin, M.-H.; Srivastava, S.; le Noble, W. J. *J. Am. Chem. Soc.* **1986**, 108, 1598.
- (16) Alabugin, I. V.; Gilmore, K. M.; Peterson, P. W. *WIREs Comput. Mol. Sci.* **2011**, 1, 109–141.
- (17) (a) Adcock, W.; Head, N. J.; Lokan, N. R.; Trout, N. A. *J. Org. Chem.* **1997**, 62, 6177. (b) Adcock, W.; Trout, N. A. *Chem. Rev.* **1999**, 99, 1415. (c) Adcock, W.; Trout, N. A. *J. Phys. Org. Chem.* **2007**, 20, 791.
- (18) Reed, A. E.; Weinstock, R. B.; Weinhold, F. *J. Chem. Phys.* **1985**, 83, 735.
- (19) (a) Alabugin, I. V.; Manoharan, M. J. *Org. Chem.* **2004**, 69, 9011. (b) Duddeck, H. *Tetrahedron* **1978**, 34, 247. (c) Muller, P. *Pure Appl. Chem.* **1994**, 66, 1077 (glossary of terms used in physical organic chemistry (IUPAC Recommendations 1994) p 1123).
- (20) Hrišl-Starčević, S.; Majerski, Z. *J. Org. Chem.* **1982**, 47, 2520.
- (21) (a) Bobek, M. M.; Brinker, U. H. *J. Am. Chem. Soc.* **2000**, 122, 7430. (b) Knoll, W.; Bobek, M. M.; Kalchauer, H.; Rosenberg, M. G.; Brinker, U. H. *Org. Lett.* **2003**, 5, 2943.
- (22) (a) Udding, A. C.; Strating, J.; Wynberg, H.; Schlattmann, J. L. M. A. *Chem. Commun.* **1966**, 657. (b) Shustov, G.; Liu, M. T. H. *Can. J. Chem.* **1998**, 76, 851. Level of theory: UB3LYP/6-311++G(3df,2pd)//UB3LYP/6-31+G(d)+ 0.98 × ΔZPVE.
- (23) (a) Isaev, S. D.; Yurchenko, A. G.; Stepanov, F. N.; Kolyada, G. G.; Novikov, S. S.; Karpenko, N. F. *Zh. Org. Khim.* **1973**, 9, 724. (b) Isaev, S. D.; Kulik, N. I.; Yurchenko, A. G. *Theor. Exp. Chem. (Transl. Teor. Eksp. Khim.)* **1993**, 29, 80. (c) Kadentsev, V. I.; Chizhov, O. S.; Kolotyrykina, N. G.; Isaev, S. D.; Kozlov, O. F.; Yurchenko, A. G. *Izv. Akad. Nauk, Ser. Khim.* **1987**, 9, 2010. (d) Yurchenko, A. G.; Isaev, S. D.; Novoselov, E. F. *Zh. Org. Khim.* **1984**, 20, 222.
- (24) (a) Knoll, W.; Bobek, M. M.; Giester, G.; Brinker, U. H. *Tetrahedron Lett.* **2001**, 42, 9161. (b) Wagner, G.; Knoll, W.; Bobek, M. M.; Brecker, L.; van Herwijnen, H. W. G.; Brinker, U. H. *Org. Lett.* **2010**, 12, 332.
- (25) Adcock, W.; Cotton, J.; Trout, N. A. *J. Org. Chem.* **1994**, 59, 1867.
- (26) (a) Burgess, K.; Van der Donk, W. A.; Jarstfer, M. B.; Ohlmeyer, M. J. *J. Am. Chem. Soc.* **1991**, 113, 6139. Adcock (see ref 4b) re-evaluated the results of Xie and le Noble, who found a ratio of 45:55 in favor of the *syn*-product: (b) Xie, M.; le Noble, W. J. *J. Org. Chem.* **1989**, 54, 3836.
- (27) (a) Dannenberg, J. J. *Chem. Rev.* **1999**, 99, 1225. (b) Fort, R. C. Jr.; Schleyer, P. v. R. *Chem. Rev.* **1964**, 64, 277. (c) Bartmess, J. E.; McIver, R. J. In *Gas Phase Ion Chemistry*; Bowers, M. T., Ed.; Academic: New York, 1979; Vol. 2, p 101.
- (28) (a) Thamattoor, D. M.; Jones, M. Jr.; Pan, W.; Shevlin, P. B. *Tetrahedron Lett.* **1996**, 37, 8333. (b) Buron, C.; Tippmann, E. M.; Platz, M. S. *J. Phys. Chem. A* **2004**, 108, 1033. (c) Lemal, D. M.; Gosselink, E. P.; McGregor, S. D. *J. Am. Chem. Soc.* **1966**, 88, 582. (d) Hartwig, J. F.; Jones, M. Jr.; Moss, R. A.; Lawrynowicz, W. *Tetrahedron Lett.* **1986**, 27, 5907. (e) Doering, W. v. E.; Hoffmann, A. K. *J. Am. Chem. Soc.* **1954**, 76, 6162. (f) Hine, J. *J. Am. Chem. Soc.* **1950**, 72, 2438. (g) Hine, J.; Dowell, A. M. Jr. *J. Am. Chem. Soc.* **1954**, 76, 2688. (h) Brinker, U. H.; Ritzer, J. J. *J. Am. Chem. Soc.* **1981**, 103, 2116. (i) Brinker, U. H.; Miebach, T. *J. Org. Chem.* **1999**, 64, 8000. (j) Nordvik, T.; Mieusset, J.-L.; Brinker, U. H. *Org. Lett.* **2004**, 6, 715.
- (29) (a) Schmitz, E. In *Chemistry of Diazirines*; Liu, M. T. H., Ed.; CRC: Boca Raton, 1987; Vol. 1, p 57. (b) Schmitz, E.; Ohme, R. *Chem. Ber.* **1962**, 95, 795. (c) Schmitz, E.; Ohme, R. *Chem. Ber.* **1961**, 94, 2166.
- (30) Moss, R. A. *Acc. Chem. Res.* **2006**, 39, 267.
- (31) (a) Maeda, Y.; Matsunaga, Y.; Wakahara, T.; Takahashi, S.; Tsuchiya, T.; Ishitsuka, M. O.; Hasegawa, T.; Akasaka, T.; Liu, M. T. H.; Kokura, K.; Horn, E.; Yoza, K.; Kato, T.; Okubo, S.; Kobayashi, K.; Nagase, S.; Yamamoto, K. *J. Am. Chem. Soc.* **2004**, 126, 6858. (b) Niino, Y.; Wakahara, T.; Akasaka, T.; Liu, M. T. H. *ITE Lett. Batteries, New Technol. Med.* **2002**, 3, 82. (c) Akasaka, T.; Liu, M. T. H.; Niino, Y.; Maeda, Y.; Wakahara, T.; Okamura, M.; Kobayashi, K.; Nagase, S. *J. Am. Chem. Soc.* **2000**, 122, 7134.
- (32) (a) Shustov, G. V.; Liu, M. T. H.; Houk, K. N. *Can. J. Chem.* **1999**, 77, 540. (b) Bonneau, R.; Liu, M. T. H. *J. Phys. Chem. A* **2000**, 104, 4115. (c) Liu, M. T. H.; Ramakrishnan, K. *Tetrahedron Lett.* **1977**, 3139. (d) Note: the substituted adamantane-derived azines consist of two isomers each.
- (33) Liu, M. T. H.; Choe, Y.-K.; Kimura, M.; Kobayashi, K.; Nagase, S.; Wakahara, T.; Niino, Y.; Ishitsuka, M. O.; Maeda, Y.; Akasaka, T. *J. Org. Chem.* **2003**, 68, 7471.
- (34) Maier, W. F.; Schleyer, P. v. R. *J. Am. Chem. Soc.* **1981**, 103, 1891.
- (35) Bally, T.; Matzinger, S.; Truttmann, L.; Platz, M. S.; Morgan, S. *Angew. Chem., Int. Ed. Engl.* **1994**, 33, 1964.
- (36) (a) Bonneau, R.; Hellrung, B.; Liu, M. T. H.; Wirz, J. *J. Photochem. Photobiol., A* **1998**, 116, 9. A singlet GS is predicted for adamantanylidene, with an S–T energy gap of 2.82 kcal/mol at the RHF/6-31G(d) and B3LYP/6-31+G(d) levels for **5b** and UHF/6-31G(d), ROHF/6-31G(d) and UB3LYP/6-31G(d) levels for **35b**. Geometries were optimized, and vibrational frequencies were determined at the DFT (B3LYP/6-31+G(d)) level to make the zero-point corrections using a scale factor of 0.95. (b) Bonneau, R.; Liu, M. T. H. *J. Am. Chem. Soc.* **1996**, 118, 7229.

(37) Here, the term antiperiplanar always refers to a hypothetical intermolecular " σ_{inc} " bond.

(38) The vacant carbene p-orbital is called lp^* in the output file of NBO analyses. It is related—but not identical with—the LUMO of **5**.

(39) (a) Carey, F. A.; Sundberg, R. J. In *Advanced Organic Chemistry, Part A, Structure and Mechanisms*, 3rd ed.; Plenum Press: New York, 1990; pp 215–216. (b) IUPAC, *Compendium of Chemical Terminology*, 2nd ed. (the "Gold Book") 1997. Online corrected version: 1994, "Curtin–Hammett principle".

(40) The FMO at the TS shows the influence of hyperconjugation on the calculated orbitals.

(41) Jones, W. M.; Brinker, U. H. In *Pericyclic Reactions*; Marchand, A. P., Lehr, R. E., Eds.; Academic: New York, 1977; Vol. 1, pp 109–198.

(42) (a) Doering, W. v. E.; Prinzbach, H. *Tetrahedron* **1959**, *6*, 24. (b) Ramalingam, M.; Ramasami, K.; Venuvanalingam, P.; Sethuraman, V. *J. Mol. Struct. (Theochem.)* **2005**, *755*, 169.

(43) Bach, R. D.; Su, M.-D.; Aldabbagh, E.; Andrés, J. L.; Schlegel, H. B. *J. Am. Chem. Soc.* **1993**, *115*, 10237.

(44) (a) Arduengo, A. J. III; Calabrese, J. C.; Davidson, F.; Dias, H. V. R.; Goerlich, J. R.; Krafczyk, R.; Marshall, W. J.; Tamm, M.; Schmutzler, R. *Helv. Chim. Acta* **1999**, *82*, 2348. (b) Mieusset, J.-L.; Brinker, U. H. *J. Org. Chem.* **2007**, *72*, 10211.

(45) The calculated TS for **5b**...CyH is ca. 10^{-2} hartree (~ 6 kcal/mol) above their combined energies.

(46) According to NBO analysis, the equatorial H atoms are slightly more positive and the axial C–H bonds are more stretched. This is reflected in the electron population of the C–H bonds $\sigma(\text{C–H})_{\text{eq}} > \sigma(\text{C–H})_{\text{ax}}$ and $\sigma^*(\text{C–H})_{\text{eq}} < \sigma^*(\text{C–H})_{\text{ax}}$.

(47) (a) Pezacki, J. P.; Wood, P. D.; Gadosy, T. A.; Lusztyk, J.; Warkentin, J. *J. Am. Chem. Soc.* **1998**, *120*, 8681. (b) Pezacki, J. P.; Shukla, D.; Lusztyk, J.; Warkentin, J. *J. Am. Chem. Soc.* **1999**, *121*, 6589. (c) Mieusset, J.-L.; Besspokoiev, A.; Pacar, M.; Abraham, M.; Arion, V. B.; Brinker, U. H. *J. Org. Chem.* **2008**, *73*, 6551.

(48) (a) Kirmse, W. In *Advances in Carbene Chemistry*; Brinker, U. H., Ed.; JAI Press: Greenwich, 1994; Vol. 1, pp 1–57. (b) Kirmse, W.; Meinert, T. *J. Chem. Soc., Chem. Commun.* **1994**, 1065. (c) Kirmse, W.; Meinert, T.; Modarelli, D. A.; Platz, M. S. *J. Am. Chem. Soc.* **1993**, *115*, 8918. (d) Holm, K. H.; Skattebøl, L. *J. Am. Chem. Soc.* **1977**, *99*, 5480. (e) Knoll, W.; Mieusset, J.-L.; Arion, V. B.; Brecker, L.; Brinker, U. H. *Org. Lett.* **2010**, *12*, 2366.

(49) Intramolecular insertion product **7** should be formed by a protic mechanism, because its formation is a thermal reaction with a high activation barrier.

(50) Structures determined using 2-D NMR; cf. Lenoir, D.; Hall, R. E.; Schleyer, P. v. R. *J. Am. Chem. Soc.* **1974**, *96*, 2138.

(51) (a) Steenken, S. *Pure Appl. Chem.* **1998**, *70*, 2031. (b) Bethell, D.; Newall, A. R.; Stevens, G.; Whittaker, D. *J. Chem. Soc., B* **1969**, 749. (c) Bethell, D.; Newall, A. R.; Stevens, G.; Whittaker, D. *J. Chem. Soc., B* **1971**, 23.

(52) A radical recombination mechanism (not shown) may be dismissed for singlet reactions of carbene **5**.

(53) Thus, one could portray such carbenes as $\pm \text{CR}_2$.

(54) Pliego, J. R. Jr.; De Almeida, W. B. *J. Phys. Chem. A* **1999**, *103*, 3904.

(55) (a) Mieusset, J.-L.; Brinker, U. H. *J. Am. Chem. Soc.* **2006**, *128*, 15843. (b) Mieusset, J.-L.; Brinker, U. H. *J. Org. Chem.* **2006**, *71*, 6975.

(56) (a) Bordwell, F. G.; Satish, A. V. *J. Am. Chem. Soc.* **1991**, *113*, 985. (b) Washabaugh, M. W.; Jencks, W. P. *Biochemistry* **1988**, *27*, 5044.

(57) (a) Liu, M. T. H.; Subramanian, R. *J. Chem. Soc., Perkin Trans. 2* **1986**, 1233. (b) Kirmse, W.; Lelgemann, R.; Friedrich, K. *Chem. Ber.* **1991**, *124*, 1853. (c) Warner, P. M.; Chu, I.-S. *J. Am. Chem. Soc.* **1984**, *106*, 5366. (d) Turro, N. J.; Cha, Y.; Gould, I. R. *Tetrahedron Lett.* **1985**, 5951.

(58) Mieusset, J.-L.; Brinker, U. H. *Eur. J. Org. Chem.* **2008**, 3363.

(59) Pezacki, J. P.; Warkentin, J.; Wood, P. D.; Lusztyk, J.; Yuzawa, T.; Gudmundsdottir, A. D.; Morgan, S.; Platz, M. S. *J. Photochem. Photobiol., A* **1998**, *116*, 1.

(60) Initially, a more stable complex is formed. The following TS is still more stable than the energy of the reactants combined.

(61) Except for carbene **5h**, NBO analysis of each $\text{MeO}\cdots\text{H}\cdots\text{5}$ TS attributed the H atom to the C atoms of the carbene **5** moieties. According to gas-phase calculations, the H atom of the inserted O–H bond is protic and the interaction with the carbene **5** lp is dominant. No Felkin–Anh-type interaction is found whenever the NBO analysis attributes the H atom from MeOH onto the adamantanylidene moiety, which confers a partial positive charge onto the formerly divalent C atom. However, the usefulness of gas-phase computations for $\text{TS}(\mathbf{5} \rightarrow \mathbf{9})$ is questionable, because they overemphasize concerted mechanism **2**. Therefore, further calculations including solvent effects are welcome.

(62) Solution dynamics are expected to be more complex.

(63) Kano, D. Ph.D. Dissertation, The University of Tokyo, Japan, 2001.

(64) (a) When ΔE_{cat} and ΔE_{carb} values (differences of the conformer energies) are plotted instead of electronegativities, the same substituent is not at the same point of the x-axis. (b) Probably also in case of the corresponding cations **6**.

(65) Gaussian 03: Frisch, M. J. et al. Gaussian, Inc., Pittsburgh, PA, 2003.

(66) (a) Becke, A. D. *J. Chem. Phys.* **1993**, *98*, 5648. (b) Lee, C.; Yang, W.; Parr, R. G. *Phys. Rev. B* **1988**, *37*, 785.

(67) (a) Mendez, F.; Garcia-Garibay, M. A. *J. Org. Chem.* **1999**, *64*, 7061. (b) Schreiner, P. R. *Angew. Chem., Int. Ed.* **2007**, *46*, 4217.

(68) (a) Kira, M.; Akiyama, M.; Ichinose, M.; Sakurai, H. *J. Am. Chem. Soc.* **1989**, *111*, 8256. (b) Schleyer, P. v. R.; Nicholas, R. D. *J. Am. Chem. Soc.* **1961**, *83*, 182. (c) Cuddy, B. D.; Grant, D.; Karim, A.; McKervey, M. A.; Rea, E. J. *J. Chem. Soc., Perkin Trans. I* **1972**, 2701. (d) Geluk, H. W.; Schlattmann, J. L. M. A. *Recl. Trav. Chim. Pays-Bas* **1969**, *88*, 13. (e) Bone, J. A.; Whiting, M. C. *J. Chem. Soc., Chem. Comm.* **1970**, 115. (f) Molle, G.; Dubois, J. E.; Bauer, P. *Can. J. Chem.* **1987**, *65*, 2428. (g) Loomes, D. J.; Robinson, M. J. T. *Tetrahedron* **1977**, *33*, 1149.

(69) (a) Bobek, M. M. Ph.D. Dissertation, University of Vienna, Austria, 2000. (b) van Herwijnen, H. W. G. Ph.D. Dissertation, University of Vienna, Austria, 2002.

(70) Calibrated to solvent residual peak at $\delta_{\text{H}} = 7.28$ ppm.

(71) Calibrated to solvent residual peak at $\delta_{\text{C}} = 127.77$ ppm.

(72) For ketone **4c**, see refs 68b and 68c. Ketone **4c** was synthesized either from alcohol **10** (12% yield) or from adamantane **12** (7% yield) and was contaminated with up to 3% of **4b** and dimethyladamantanone. Hence, these byproducts were carried along during the synthesis and reactions of 3*H*-diazirine **1c**.

(73) Bobek, M. M.; Brinker, U. H. *Synth. Commun.* **1999**, *29*, 3221.

(74) (a) Nelsen, S. F.; Klein, S. J.; Trieber, D. A. II; Ismagilov, R. F.; Powell, D. R. *J. Org. Chem.* **1997**, *62*, 6539. (b) UV(C_6H_{14}): λ_{max} ($\epsilon \times 10^4$): 211 (25), 232 (7.7); melting was not observed up to 260 °C; compound **3h** seems to melt and to sublime at this temperature simultaneously.